HIGH TEMPERATURE EROSION WEAR OF TiCN-BASED CERMETS

A DISSERTATION

Submitted in partial fulfillment of the

requirements for the award of the degree

of

MASTER OF TECHNOLOGY

in

DEPARTMENT OF METALLURGICAL AND MATERIALS ENGINEERING

(With Specialization in Industrial Metallurgy)

by

DINESH SINGH

DEPARTMENT OF METALLURGICAL AND MATERIALS ENGINEERING

INDIAN INSTITUTE OF TECHNOLOGY ROORKEE

ROORKEE – 247667 (INDIA)

MAY, 2016

CANDIDATE'S DECLARATION

I hereby declare that the work presented in this dissertation entitled "**High temperature Erosion wear of TiCN-based cermets"** in partial fulfillment of the requirement for the award of the degree of **Masters of Technology** in **Metallurgical and Materials Engineering** with specialization in **Industrial Metallurgy,** submitted in the **Department of Metallurgical and Materials Engineering, Indian Institute of Technology, Roorkee** is an authentic record of my own work carried out during the period from July 2015 to May 2016 under the supervision of **Dr. B.V. Manoj Kumar,** Associate Professor, Department of Metallurgical and Materials Engineering, Indian Institute of Technology, Roorkee.

The matter presented in this dissertation to the best of my knowledge has not been submitted by me for the award of any other degree elsewhere.

Dated: May 26, 2016

Place: Roorkee **DINESH SINGH**

(14544004)

CERTIFICATE

This is to certify that above statement made by the candidate is correct to the best of my knowledge and belief.

Dr. B.V. Manoj Kumar
Associate Professor,
MMED, IIT Roorkee
Roorkee-247667 (INDIA)

ACKNOWLEDGEMENT

I would like to thank the almighty God for his protection and giving me peace throughout my work. I am highly indebted to **Dr. B.V. Manoj Kumar,** Associate Professor, Department of Metallurgical and Materials Engineering, Indian Institute of Technology Roorkee, for encouraging me to undertake this dissertation as well as providing me all the necessary guidance and inspirational support throughout this dissertation work. He has displayed unique tolerance and understanding at every step of progress. It is my proud privilege to have carried out this dissertation work under his able guidance.

I wish to express my sincere thanks to **Dr. Anjan Sil,** Professor and Head of the Department, Metallurgical and Materials Engineering Department, Indian Institute of Technology Roorkee, for his help to carry out this dissertation.

I would also like to express sincere thanks to **Dr. S.R. Meka,** Assistant Professor, Department of Metallurgical and Materials Engineering, Indian Institute of Technology Roorkee, for providing valuable suggestions in X-ray diffraction analysis.

I also like to express my gratitude to Mr. Sandan Kumar Sharma, Dr. Ashish Selokar, Dr.Vipin Sharma, Yashpal and Vikash verma , Research Scholar for their innumerable discussion, his generosity and willingness to share his knowledge. I sincerely appreciate his valuable persistent encouragement in making this work.

I would also like to express my special thanks to Mr. Kapil, Mr. Atul Chaudhary, Mr. Abhishek Gupta, Mr. Rakesh Ahlawat and Mr. Diwan singh chauhan for their scientific, financial and moral help, inspiration, and valuable suggestions throughout the tenure.

I would like to acknowledge all my friends for their valuable information share, and developing love and confidence in me throughout the work. Last but not the least I would like to thanks my parents and my brother who have been a constant source of my inspiration to me.

ABSTRACT

In order to improve wear resistance of cermets for the use in cutting tool applications, development of new compositions is necessary. The purpose of the preset work is to prepare dense TiCN-10 wt% Mo_2C-10 wt%WC-10 wt%Ni-10 wt% Co cermets with restricted coarsening by ball milling and spark plasma sintering and estimate the potential of the sintered cermets in erosion wear conditions. The reduction of commercially available TiCN and Mo_2C powders by milling and further mixing with other constituents for 8 to 72 h resulted in oxidation products. Spark plasma sintering at 1200- 1300^oC and 40-50 MPa resulted in 97-98% dense cermets. The microstructure of the developed cermets reveals black core of TiCN, white cores and grey rim of (Ti, W, Mo)CN. Typical hardness of 10.48 GPa and fracture toughness 9.44 $MPam^{1/2}$ are obtained for cermets sintered using 72 h mixed powders. Erosion by SiC particles of at normal incidence reveals removal of binder phase and pull-out or fracture of ceramic grains. At elevated temperature of 400^oC, easy removal of binder phase resulted in increased fracture of ceramic grains, leading to 1.5 to 2 times erosion compared to erosion at room temperature.

TABLE OF CONTENTS

LIST OF FIGURES

LIST OF TABLES

LIST OF ABBREVIATIONS

SEM – Scanning electron microscopy

TEM – Transmission electron microscopy

XRD – X-ray diffraction

EDX – Energy dispersive X-ray spectroscopy

SPS – Spark plasma sintering

UHV – Ultra high vacuum

COF – Coefficient of friction

T8 – 8 hour mixed powder

T48 – 48 hour mixed powder

T72 – 72hour mixed powder

CHAPTER 1 INTRODUCTION

1.1 Cermets

Cermets are the composite materials consisting ceramic (cer) and metallic (met) materials. Cermets incorporate the desirable properties and suppress undesirable properties of both metals and ceramics. Till date, cermets have been advised as the most auspicious materials for high speed cutting tools compared to the other carbides and metals because of their high hot hardness, low thermal expansion coefficient, good wear resistance and high thermal conductivity [1]. A high thermal conductivity cermets would decrease temperature gradient at high temperature and also decreases thermal stress and thermal shock induced cracks generated during machining [2]. There are mainly two types of cermets: conventional and advanced cermets.

WC-Co based hard materials are known as conventional cermets. Traditional cermets (WC-Co alloys) are tough and hard but properties of these cermets suddenly decline at high speed cutting, may be because of their inferior oxidation resistance and plastic deformation at elevated temperature [3].

Conventional WC-based hard metals are being replaced by advanced cermets because of their superior properties such as improved surface finishing, provide geometrical accuracy, increase the cutting speed [2].

In recent time, there are two types of cermets available, mainly titanium carbide (TiC)-based and titanium carbo-nitride (TiCN)-based cermets are being preferred for cutting tool inserts. Compared to the TiC-based cermets, hot hardness, transverse rupture strength, oxidation resistance, wear resistance, chemical and thermal stability at elevated temperature are high for TiCN-based cermets have much higher. Also, the coefficient of thermal expansion is less. It is more important that they are less expensive and light weight than WC-Co based hard metal but they suffer because of their brittle nature [1-2,4]. Major properties of TiC and TiCN cermets at high temperature are listed in **Table1.1**.

Furthermore, creep deformation resistance for TiCN-based cermets at high temperature is better than that for TiC-based cermets. Therefore, built-up edges, scaling or oxide layer formation tends to be difficult in case of TiCN-based cutting tools. This can be ascribed for the higher values of enthalpy of formation of TiCN [1].

Table 1.1. Summary of properties of TiC and TiCN based cermets at elevated temperatures[2].

Cermets	**TiC-based cermets**	**TiCN-based cermets**
Micro hardness (MPa)	4090 at 1000 ^{o}C	5883 at 1000 ^{o}C
Transverse rupture Strength (MPa)	1050 at 900 °C	1360 at 900 °C
Weight gain (mg/cm^2/h)	11.8 at 1000 °C	1.6 at 1000 °C
Thermal conductivity (W/m/K)	24.7 at 1000 °C	42.3 at 1000 °C

TiCN based cermets consist of hard ceramic phase, titanium carbo-nitride (TiCN) as the principal component, and additional metal secondary carbides of the VB or VIB groups, like VC, HfC, NbC, TaC, Mo_2C and WC etc to enhance the sinterability. A metal as a binder phase such as nickel, cobalt, molybdenum and nickel–cobalt gives desired adhesion of the hard particles and desired toughness[1].

In general, TiCN based cermets are mainly composed of three categories of phases: ceramic as a hard phase (core), surrounding phase (rim) and metal binder phase. As reported in literature, usually there is core-rim type structure but at some times, the rim is divided into two layers, known as the inner rim which is formed during solid state sintering by diffusion and the outer rim, which is formed during liquid phase sintering by dissolution re-precipitation of secondary carbides [2,5,6].

During liquid phase sintering consolidation, a typical core-rim structure **(Fig.1.1)** is developed, in which the core consists of the partially dissolved TiCN hard particles, and the rim consists of a newly formed typical carbo-nitride solid solution containing titanium and other secondary carbides by dissolution and re-precipitation reaction [5,7].

Two types of grains in the cermets have been noted: one is fine black core and grey rim type structure, another is obvious white core and grey rim type structure [5,6,8,9].

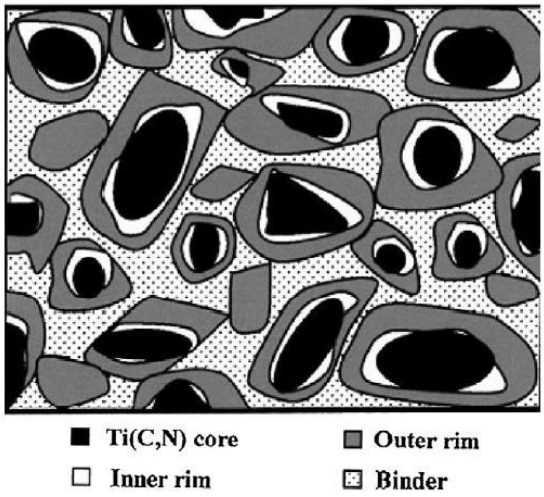

Fig. 1.1. Schematic microstructure of TiCN based cermets[1].

TiCN has a face centered cubic (fcc), NaCl type structure. TiCN is a solid solution of TiC and TiN. If there are no vacancies of C or N atoms, the structure will be of tetragonal, otherwise fcc[1].

As per the Hall-Patch relation, ultrafine grain materials have improved properties. For improving efficiency of cermets cutting tools, significant research studies conducted to develop TiCN-based cermets with ultrafine structures Four principle ways of preparing nano or ultrafine powders of TiCN are generally reported, namely self propagating reaction at high temperature synthesis, carbo-thermal reduction synthesis, and mechanically-induced self-sustaining reaction, chemically synthesis and ball-milling [1,2,5].

It is well known that sintering plays very important role for consolidation of TiCN-based cermets. The long duration of sintering in conventional sintering techniques limits preparation of nano sized or ultrafine. In this regard, rapid sintering techniques like field assisted sintering technique or spark plasma sintering(SPS) give an advantage by employing high heating rates to prepare TiCN-ultrafine powder to full density in a short span of time, restricting the growth of grains[6].

As the nose of the cutting tool insert during machining is subjected to friction induced temperatures, it becomes necessary to design a composition of the cermets that exhibits superior wear resistance at high temperatures[10]. In this regard, studies have been done to study the performance of TiCN based cermets in varieties of wear contacts, namely fretting, sliding, erosion or crater wear. It is reported that the following wear mechanisms occur simultaneously during wear: (i) abrasion on either or both of the tool and work piece, material transfer or adhesion and diffusion of chemical species in rubbing or chipping, leading to tribo-chemical wear [10,11,12].

Erosion may be defined as material removal process from a surface due to the interaction between surface and fluid, or impinging solid or liquid particles. Erosive wear is possible to occurred by the impact of solid or liquid particles against the cermets surface during machining operations [2,11,12]. Considering the fact that Mo_2C addition restricts the grain coarsening [5,9,13-15], the proposed research aims to develop new ultrafine composition of TiCN-WC-Mo_2C-Ni-Co cermet system by spark plasma sintering for their use in high temperature wear applications.

Objectives of the thesis:

The major objectives of the thesis are as follows:

(i) To reduce particle size of TiCN and other ceramic particles by comminution using ball milling and mixing powders

(ii) To optimize spark plasma sintering operating conditions to obtain fully dense cermets system with ultrafine crystallites.

(iii) To study microstructural and mechanical characteristics of sintered cermets

(iv) To study behavior of sintered cermets in ambient and high temperature (400^oC) erosion conditions

(v) To understand the wear mechanisms of the cermets system.

Structure of the thesis:

The thesis is divided into the following chapters:

Chapter 1 Introduction of ultrafine TiCN-based cermets.

Chapter 2 deals with the available literature on sintering TiCN-based cermets and tribological characteristics. Details of ball milling, spark plasma sintering experiments and erosion testing are explained in **Chapter 3**. The surface analysis of the sintered and worn surfaces is also provided. The major results from ball milling, spark plasma sintering and erosion testing are provided in **Chapter 4**. This is followed by detailed discussion of the results in the same chapter. **Chapter 5** deals with the major conclusions from the present work and scope for the future work. **Chapter 6** deals with scope of future work and **Chapter 7** includes References.

2.1 Titanium carbo-nitride (TiCN)

Generally, the titanium carbo-nitride (TiCN) is a non-oxide material which is a continuous solid solution of TiC and TiN, hence the properties of TiCN depends on both TiC and TiN [1,3,7]. In the lattice, structure the C atoms in the Ti lattice can be reside by N in any ratio. Titanium carbo-nitride (TiCN) has a face centered cubic (fcc), NaCl type structure. Generally if there is some vacancy of C and N atoms, then the structure is of fcc type, otherwise tetragonal [1]. It was stated that ceramics, very broadly speaking, can be considered to be either ionically or covalently bonded (in **Fig.2.1**) [42].

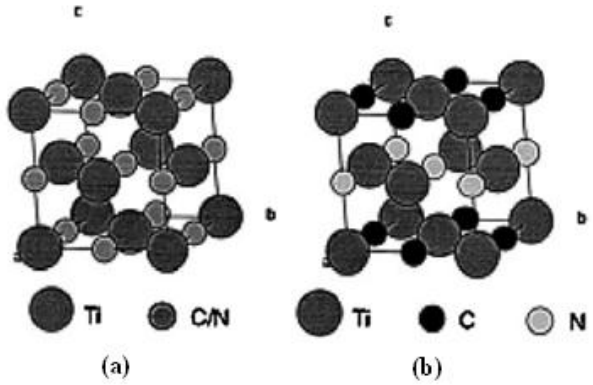

Fig. 2.1. Structures of TiCN: (a) With C and N vacancy (b) Without C and N vacancy [1]

2.1.1 Mechanical properties of TiCN

TiCN possess the properties of both TiC and TiN eg., high melt point, hardness, electric/thermal conductivity at elevated temperature, superior resistance against corrosion and wear, better chemical stability (**Table 2.1**) [1-19].

Table 2.1 Typical properties of TiC, TiN and TiCN ceramics [2]

Material	**Density (gm/cc)**	**Melting point (°C)**	**Thermal conductivity at 20 °C (W/m* K)**	**Coefficient of thermal expansion (10^{-6} /K)**	**Vickers hardness (GPa)**	**Crystal structure**
TiC	4.90–4.93	3257	17-24	7.40–7.95	30-32	fcc
TiN	5.39–5.44	2950	29	9.35	20	fcc
TiCN	5.08	2000	42.3	-	-	fcc, (NaCl type) or tertragonal

2.1.2 Applications of TiCN

Major engineering applications of TiCN-based cermets are in high speed cutting tools materials. TiCN-based cermets also used as high speed milling and finishing processes, in die making and dentistry, (see **Fig.2.2)** [1-19].

Fig. 2.2. Applications of TiCN-based cermets [https://wikipedia.org/Titanium nitride]

2.2 Effect of C and N on TiCN-based cermets

Peng Y. *et al.* reported that the C/N ratio plays a significant role on the particle size of Ti(C_XN_Y)-based cermets. And it was studied that as the amount of nitrogen content increases, then stability of Ti(C_{1-X} N_X) is increased up to 1500°C, due to the relative stability of TiC and TiN. As the amount of nitrogen content increases then the free energy of formation of Ti(C_{1-X} N_X) decreases According to the thermodynamic calculations, Ti($C_{0.3}N_{0.7}$) and Ti($C_{0.5}N_{0.5}$) are more stable than Ti($C_{0.7}N_{0.3}$) at 1500°C [2].

Kang S. *et al.* reported that TiN is higher stable phase among various Ti(C_{1-X} N_X) compositions up to 1000°C and beyond that equilibrium is shifted towards the TiC phase side. As per the Gibbs free energy of formation, the highest stability is observed at 1700K and 2100K, at nitrogen concentrations in the Ti(CN) around 0.6 and 0.3, respectively [7].

Kang S. *et al.* reported that the effect of nitrogen is much powerful in refining (Ti, W)C-based cermets than that of a Mo_2C addition due to the more affinity between carbon and nitrogen in the system [4].

2.3 Compositional design of cermets

The properties of TiCN-based cermets can be balanced by adding secondary carbides and metal binders to fulfill the requirements of the high speed cutting operations

(Fig.2.3). As TiC and TiN contents increase, hardness of the cermets increases. Additions of TaC or NbC in the TiC or TiCN improve cutting performance, whereas densification improves with the addition of WC or Mo_2C with the during sintering. For higher TiN contents, higher sintering temperature is required for consolidation of fully dense cermets without residual porosity [8].

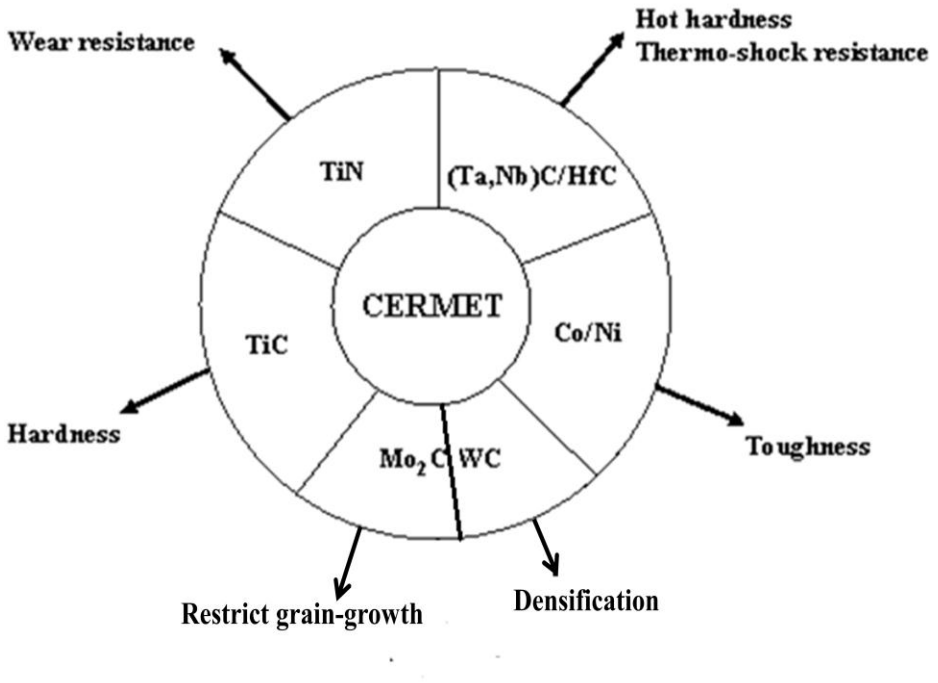

Fig. 2.3. Properties of cermets as a function of composition [8]

2.4 Influence of binder metals

As reported in the literature, binder metals have great impact on the toughness of the cermets. Cordoba *et al*. reported that nickel, cobalt or nickel and cobalt metal binders provide the desired combination of hard and tough phases [9,40]. Rajabi *et al.* reported in his paper that mechanical properties of cermets largely sustained on the metallic binder composition. Various elements such as Cr, Co, Ni, Mo, and Ni-Co could be used as a binder metal in case of TiCN-based cermets [6,13].

2.4.1 Cobalt binder

Peng *et al.* reported that cobalt (Co) binder provides higher toughness, oxidation resistance and also increases the wetting in the hard phase in the TiCN-based cermets than that of Ni.In TiCN-based cermets Ni is superior to Co for corrosion resistance [2].

2.4.2 Nickel binder

Rajabi *et al.* reported that Ni is one of the remarkable binders and has wide range of applications [6]. If Ni content in TiCN-Ni-Mo cermets increases then bending strength increases and hardness decreases [2].

Ni-binder is responsible for providing toughness, ductility and also useful in densification than Co binder. By forming single stoichiometric ratio in the TiC cermets (Ti/C: 1/1), and therefore prevent abrasion during ball-milling, Literature also revealed that Ni can be used to improve wear resistance as shown in the (**Fig.2.4(a)**) . Ti(CN)-based cermets have the maximum fracture toughness value at 20% and 25% binder content and decreases as the binder amount increases as shown in the (**Fig.2.4(b)**). Stresses induced due to thicker metal layer between ceramic particles so crack propagation is easy and hence decrease in fracture toughness is observed **Fig.2.4(c)** [6].

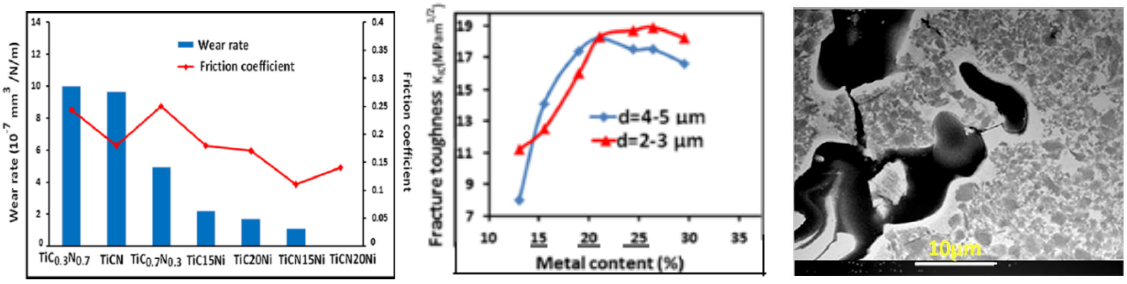

(a) (b) (c)

Fig. 2.4. (a) COF and wear rate (b) Variation of fracture toughness binder content (c) FE-SEM of crack generating path in 33 wt% of binder content [6]

2.4.3 Molybdenum (Mo) binders

As reported in the literature that Mo is introduced because of the poor wetting action of Ni binder with TiC and TiCN [2]. Rajabi *et al.* reported recently that addition of Mo as a binder can enhance the mechanical characteristics of TiC and TiCN-based cermets can be explained in this way,

(I) Addition of Mo as a binder, enhance the wettability between the ceramic phase and binder by formation of the Mo-rich shell, which enclosed the whole TiC or TiCN particle. Therefore it can decrease the angle of contact between ceramic particles and liquid phase as shown in the **Fig.2.5.**

(II) Addition of Mo as a binder decreases the solubility between ceramic particles (TiC or TiCN) and binder therefore grain growth can be restricted during sintering. Since Mo-rich exterior has less solubility in the metal binder phase than TiC or TiCN phase therefore the dissolution re-precipitation reaction was obstructed by the deficiency of ceramic particles in the binder [6].

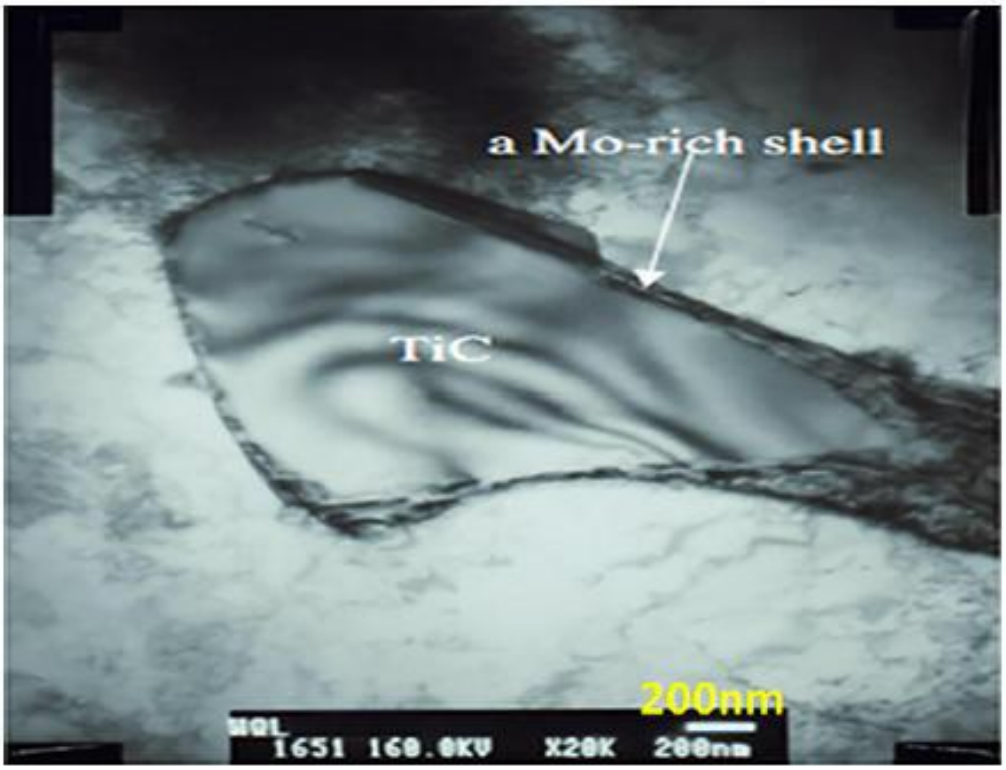

Fig. 2.5. TEM image of Mo-rich shell around TiC in (Al-0.6Cu-0.6 Mg-1.2Si-0.25Mn-10TiC-1Mo) [6]

2.4.4 Ni–Mo binders

To select the exact batch composition of Ni-Mo as a binder in cermets is still a question to the researchers. Addition of Mo restrict the grain growth therefore hardness increases. Because of high hardness the rate of wear in TiC or TiCN-based cermets enhances by increasing the Mo binder content (Ni:Mo =1:1) particles as shown in **Fig.2.6** [6].

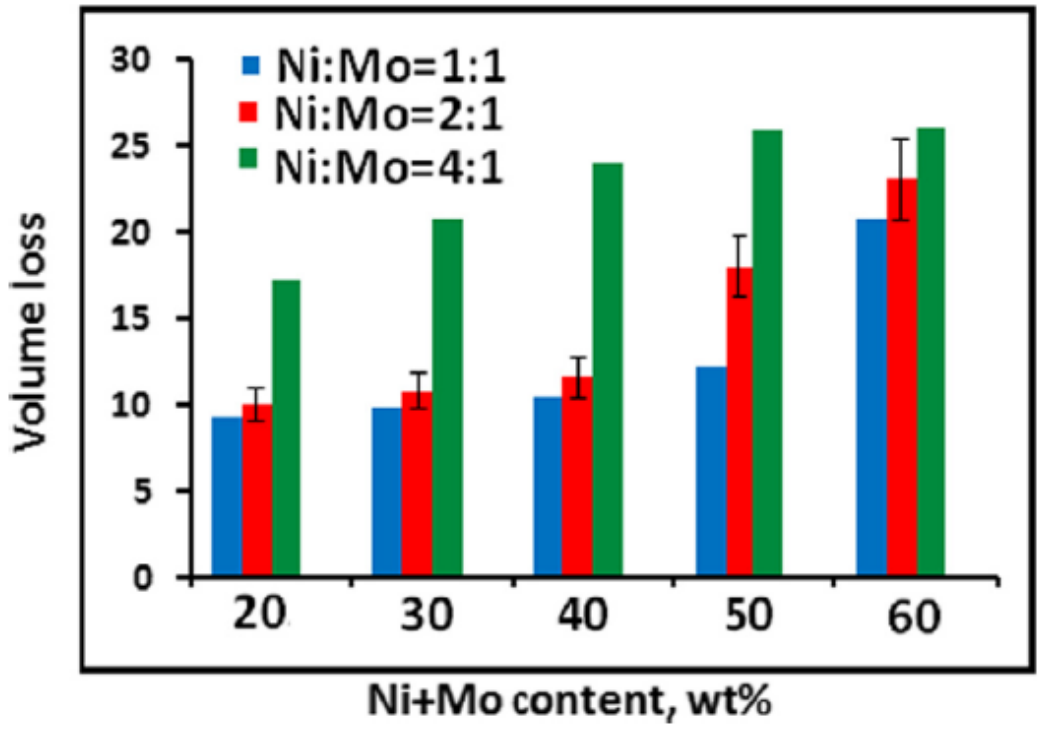

Fig. 2.6. Wear coefficient vs binder content of composites [6]

2.5 Development of Ultrafine cermets by using secondary carbides

TiCN based cermets consist of hard ceramic phase, titanium carbo-nitride (TiCN) as the principal component, and additional metal secondary carbides of the VB or VIB groups such as WC, VC, NbC, Cr_3C_2 , TaC, Mo_2C etc. to enhance the sinterability. Secondary carbides increase the wettability and fracture toughness of the cermets in order to meet particular needs during high speed cutting operations.

As reported in the literature that less stability of the secondary carbides are responsible for high wetting action between the ceramic phase and binder phase. The wetting action is highly dependent on the formation enthalpy of the cemented carbides, formation enthalpy of various carbides are listed in **Table 2.2**. As per the formation enthalpy, the additions of Mo2C and WC have great improvement in the wetting action between the hard ceramic phase and binder phase. Solubility of VC and Cr_3C_2 is much higher compare to the others in the binder phase therefore grain growth of the hard ceramic phase is restricted [2].

Table 2.2. The enthalpy of formation of secondary carbides at 298 K [2]

Carbides	TaC	NbC	VC	Cr_3C_2	WC	Mo_2C
Enthalpy of formation (KJ/mol)	−183.7	−142.3	−126.4	89.7	−35.1	−17.6

2.5.1 The effect of TaC content on ultrafine cermets

Ettmayer *et al.* reported in his paper that addition of TaC can enhance the high hot hardness and resistance against plastic deformation of high speed cutting tools at elevated temperature [2,8,10].

Xiong *et al.* studied that TaC is very significant to most of the cermets and has direct effect on the high temperature characteristics. **Fig.2.7** shows that small addition of TaC increases the bending strength but the hardness decreases immediately. Literature also reported that the formation of carbo-nitrides solid solution takes place with the addition of TaC, therefore the bending strength of cermets is increased [2,4,10].

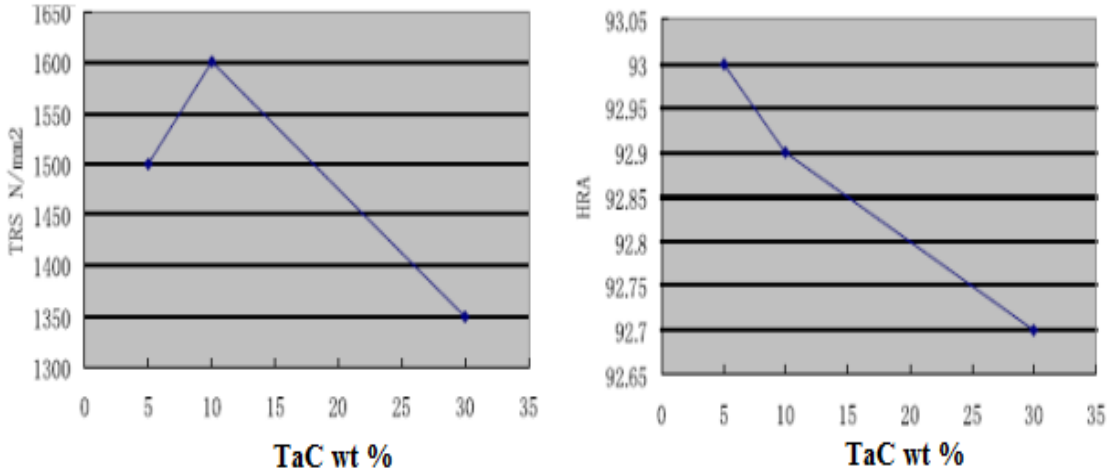

Fig. 2.7. Effect of TaC content on TRS and hardness [10]

According to the previous research the optimum amount of TaC is 7 wt% as shown in the **Fig.2.8** [8]. Highly dense cermets can be developed considerably at lower temperatures. Powdered cermets sintered at low temperature 1150°C by spark plasma sintering [11].

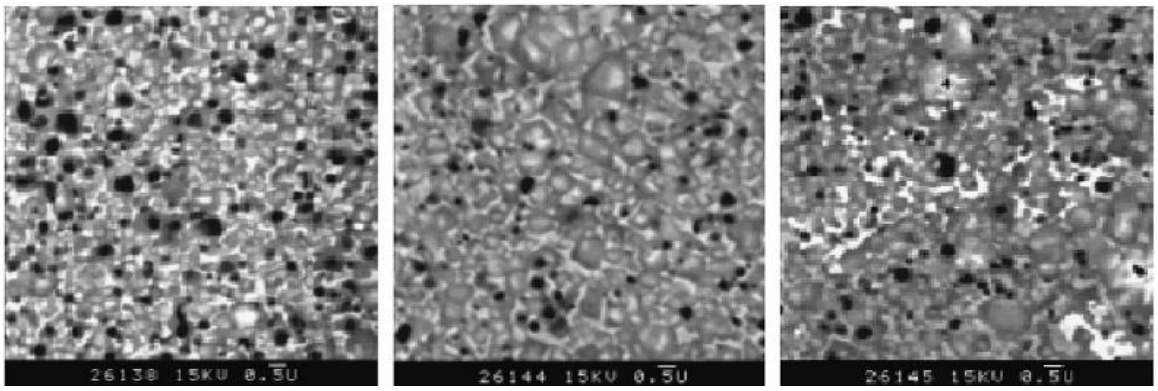

Fig. 2.8. SEM images show the effect of TaC content: (a) 5 wt% TaC; (b) 10 wt% TaC; (c) 30 wt% TaC.

Cordoba M. *et al.* reported in his paper that Nano powder $Ti_xTa_{1-x}C_{0.5}N_{0.5}$-based cermets were prepared using a mechanically induced self sustaining reaction(MSSR) and consolidated by SPS at low temperature 1150°C and also calculated the contiguity(C) of ceramic particles as follows,

$$C = 2(N_L)_{ceramic/ceramic} / (2(N_L)_{ceramic/ceramic} + (N_L)_{ceramic/binder}) \quad \ldots(2.1)$$

And mean free path(λ) of binder phase is calculated using the following equation,

$$\lambda = \varnothing_{ceramic} / (N_L)_{ceramic/binder} \quad \ldots\ldots\ldots\ldots\ldots(2.2)$$

Where,

$(N_L)_{ceramic/ceramic}$ = number of intercepts per unit length for ceramic/ceramic particles

$(N_L)_{ceramic/binder}$ = number of intercepts per unit length for ceramic/binder and

$Ø_{ceramic}$ = mean ceramic particle size.

2.5.2 The effect of NbC content on ultrafine cermets

Jun W. *et al.* reported that NbC has two effects on TiCN-based cermets; firstly it reduces the sintering temperature and also increases densification. Secondly, at the liquid phase sintering stage, almost all of the NbC dissolved into the binder phase so that amount of liquid melt increases hence densification of cermets increases. According to the literature the optimum content of NbC is 5% [2,13].

Kang S. *et al.* reported that the average dissolution rate of NbC in case of Ti($C_{0.7}$ $N_{0.3}$)-*y*NbC-20Ni system was around 1.6 times greater than that in Ti(CN) as shown in the **Fig.2.9** [4].

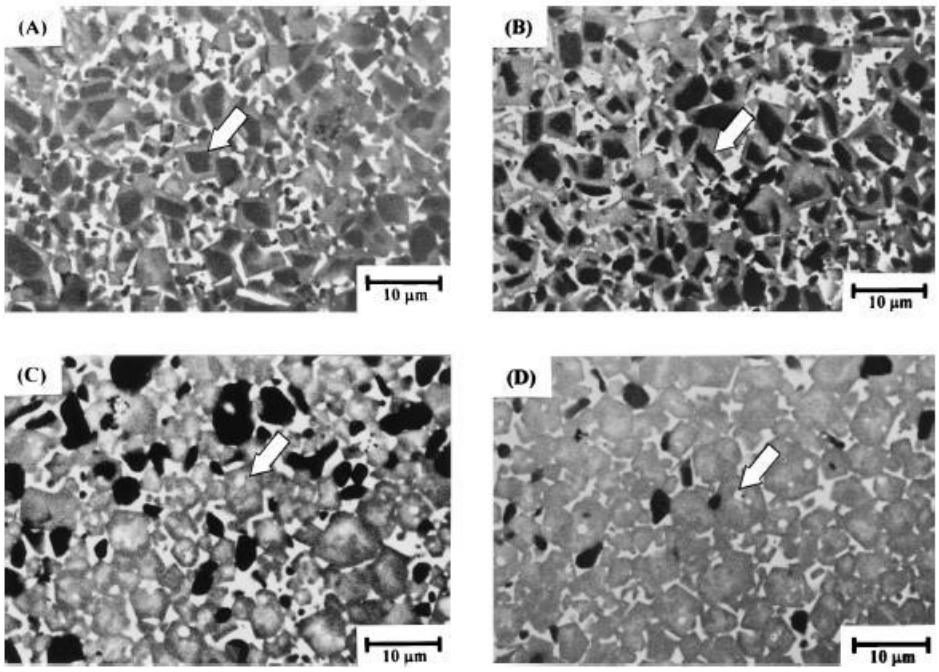

Fig. 2.9. SEM/BSE image of Ti($C_{0.7}N_{0.3}$)-*x*NbC-20Ni systems, for *x* (A) 5, (B) 10, (C) 15, and (D) 25 wt.% [4]

2.5.3 The effect of WC content on ultrafine cermets

Kang S. *et al.* reported in his paper that WC will dissolve in the liquid phase formed at the liquid sintering phase. Therefore the net amount of liquid melt increases as the addition of WC content increases. Hence the sinterability of the cermets will be improved and also the porosity decreases significantly with the increasing WC content [8,13]. As per the literature the optimum content of WC is 15% [2,10].

Kang S. *et al.* reported that Nano crystalline (Ti,W)C-Ni and (Ti ,W)(CN)-Ni powders were prepared from oxides of the respective powders and sintered at 1510°C for 1h. The resulting microstructures denote an ultrafine, coreless structure of diameter 0.5-1.0 μm. However, the fully densified cermets had a considerably enhanced toughness (11-14MPa*$m^{1/2}$). The propensity of coarsening of (Ti,W)(CN) increased because of the presence of W and Nitrogen in the cermets system [3,13].

Jun *et al.* investigated that the inner rim thickness increases with the increase of WC content. This can be explained in such a way that more amount of W dissolves in the binder phase and reacts with titanium carbo-nitride (TiCN) to form the (W, Mo)-rich inner rim when the WC content increases. The binder phase thickness decreases with the increase of WC amount. This shows that the wettability between the (Ti, Mo, W)(CN) complex solid solution and binder phase increases with the increased amount of W content in solid solution [2,4,13].

Xiong *et al.* studied that after adding small amount of WC content, the core-rim type structure becomes very typical. **Fig.2.10** shows there are three kinds of microstructures obtained,

black core + small grey rim + small white rim,

white core + small grey rim and

grey core + small white rim + small grey rim.

However, the average grain size (core + rim) of the structure obtained is smaller than that of the cermets, which have only 10 wt% Mo_2C content added. Since the hardness of the cermets can be increased by adding suitable amount of WC. But, excess addition of WC cause the precipitation of WC phase, therefore the hardness decreases.

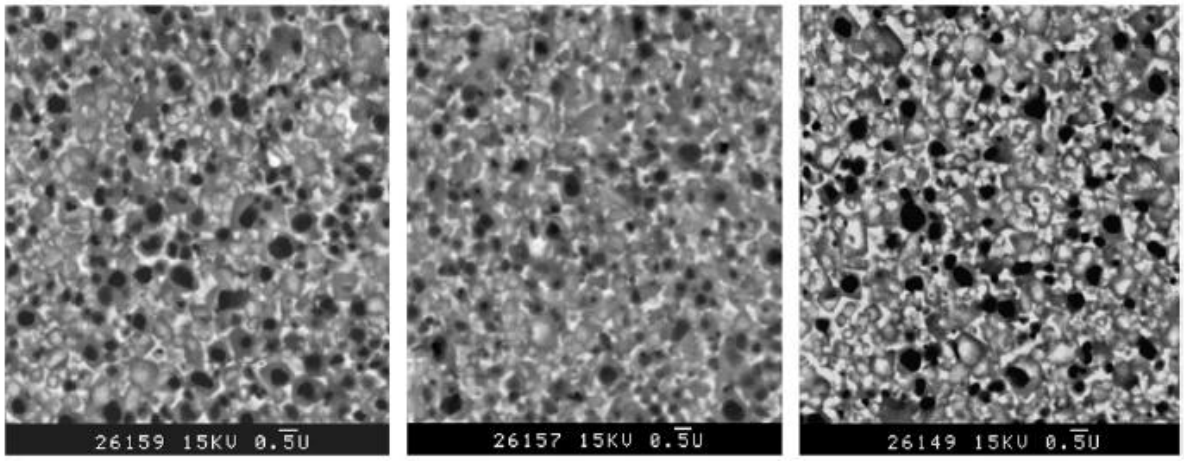

Fig. 2.10. SEM images of cermets with varying WC content: (a) 10 wt% WC; (b) 15 wt% WC; (c) 30 wt% WC.

Kang S. *et al.* reported in his research study that the TEM image of Ti($C_{0.7}N_{0.3}$)-10WC-20Ni system (in **Fig.2.11)**. Hard phases noticeable as complex core/rim structures. In the Fig. 2.11 'C', 'R' and 'B' denotes the Ti($C_{0.7}N_{0.3}$)-core, the (Ti ,W)(CN)-rim and the Ni metal binder, respectively. In general, double-layered rim structure is formed, this double layered rim is divided into two parts as inner rim and outer rim. The inner rim is close to the hard core phase and having W-rich region and the amount of W content decreases from inner to outer rim. The rate of dissolution of WC in the Ni-binder phase is greatly depends on the amount of W content in the inner rim and outer rim [8,13].

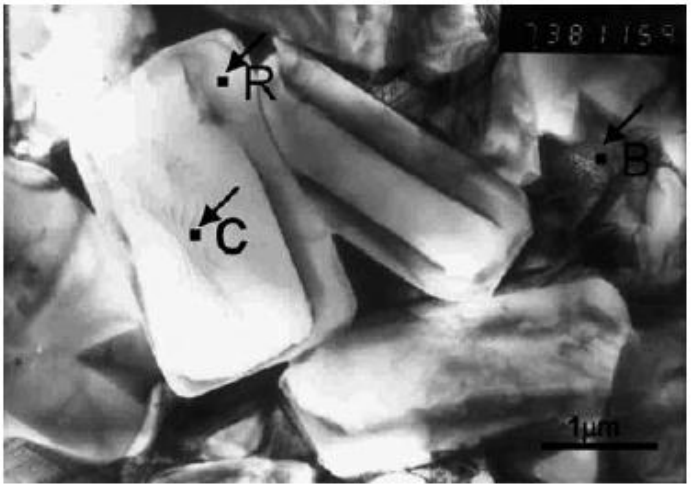

Fig. 2.11. TEM image of the Ti($C_{0.7}N_{0.3}$)-10WC-20Ni systems. 'C', 'R' and 'B' represent the 'core', 'rim' and 'binder' regions, respectively.

As reported in the literature that the bending strength can be calculated by the Griffith-Orowan equation

$\sigma = (2EP/\pi L)1/2$ .... (3)

Where, E is modulus of elasticity,

P is plastic deformation work due to crack propagation,

L is the crack length.

The Young's modulus of WC, TiC and TiN is 7.2×10^5, 3.2×10^5 and 2.51×10^5 MPa, respectively. Hence the rupture strength of cermets increases with the increased amount of WC content [8,11,12]. The optimum amount of WC for tool life and wear resistance is 10 wt.% in TiCN-20Ni-based cermets shown in **Fig.2.12(a)** and **Fig.2.12(b)** [13].

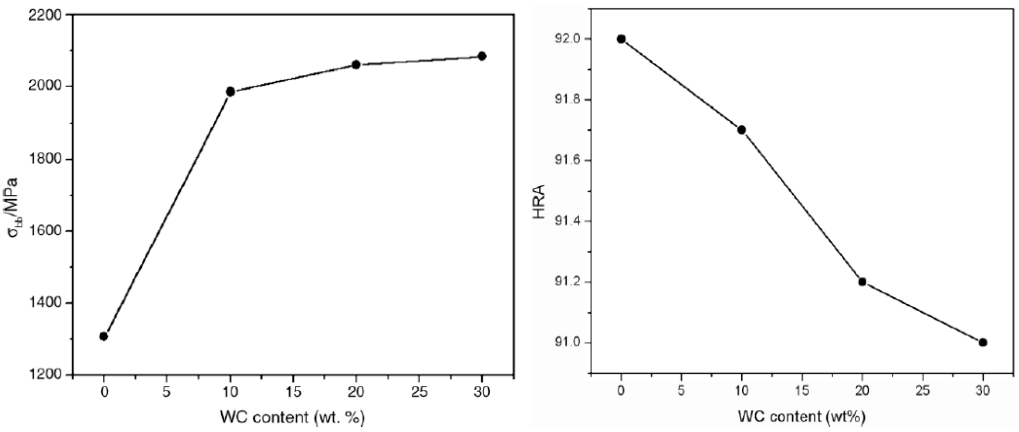

(a) (b)

Fig. 2.12. The effect of WC content on (a) TRS and (b) hardness [13]

2.5.4 The effect of Mo_2C content on ultrafine cermets

Z. Lin *et al.* reported that Mo_2C improves the wettability between the hard ceramic phase and the metallic binder phase, and simultaneously suppress the solubility of TiCN in the binder. Hence, coarsening is restricted by dissolution re-precipitation reaction during liquid phase sintering. According to the literature the optimum content of Mo_2C is 10% [2,6,8-10,13,14].

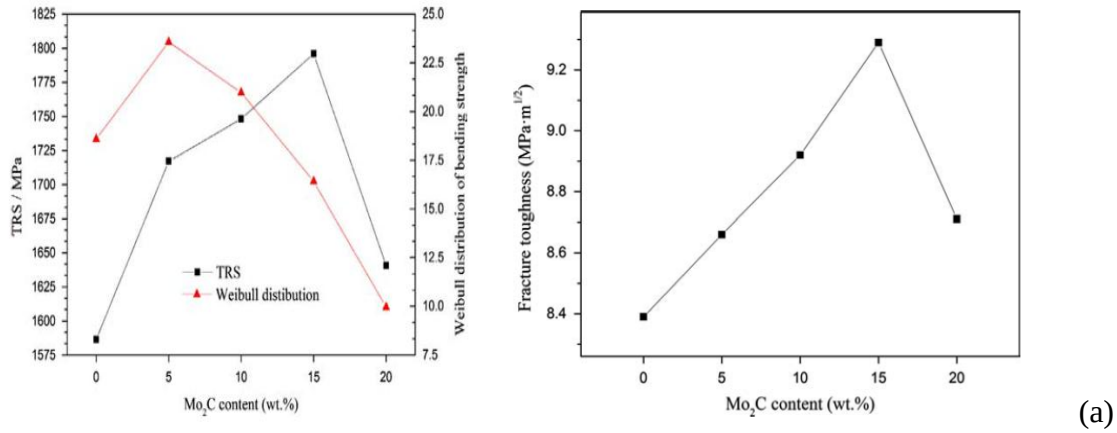

(a)

(b)

Fig. 2.13. Shows (a) TRS and Weibull distribution vs Mo_2C (b) K_{IC} versus Mo_2C content.

Mo_2C has a considerable effect on the microstructure and mechanical characteristics of the $(W_{0.5},Ti_{0.5})C$-based cermets. It is reported that the transverse rupture strength and fracture toughness are measured maximum if the Mo_2C amount is 15 wt%. After that with the further increase in Mo_2C amount, the TRS and K_{1C} decrease. It is

because of excess Mo_2C content and to increased rim thickness and brittleness Shown in the **Fig.2.13 (a)** and **Fig.2.13(b)** [8,9].

Xu Q. *et al.* reported that as the $Mo_2C/(Mo_2C+WC)$ ratio increases, then the finer TiCN grains with smaller black hard cores surrounded by thinner rim, therefore the structure of cermets tends to be more dense and having smaller binder mean free path[4,13].

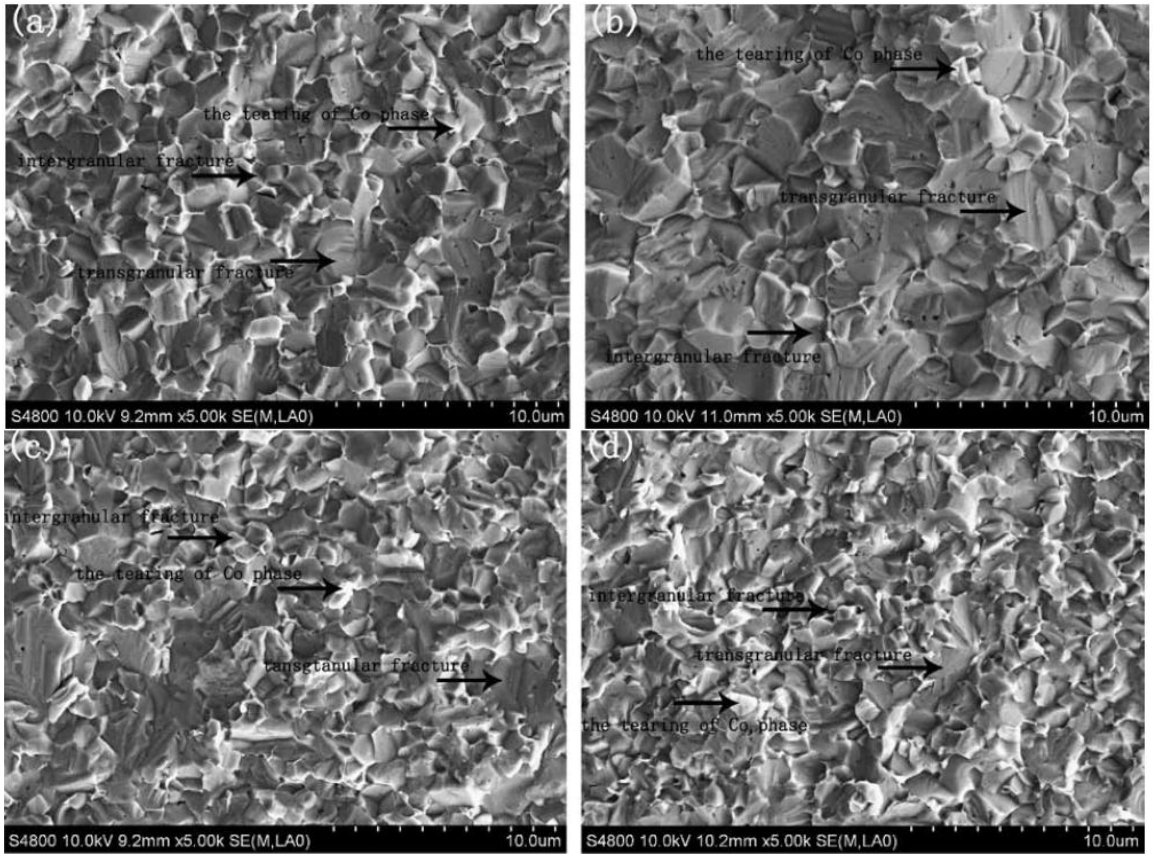

Fig. 2.14. Fracture surface of the $(W_{0.5},Ti_{0.5})C$-xMo_2C-15Co cermets: (a) x=0 wt%, (b) x=5 wt%, (c) x=10 wt.% and (d) x=15 wt%.

Genga R.M. *et al.* reported that small addition of Mo_2C carbide moderate densification while sintering (SPS) of WC-TiC-Ni cermets and for full densification higher sintering temperatures is required. The small amount addition of Mo_2C enhanced the microstructures with finer and more uniformly distributed in (Ni) binder pools [8,13,14,41].

Lin Z. *et al.* reported in his study that Due to brittle fracture mechanism of cermets, typical cleavage fracture mode is observed in (W, Ti, Mo)C grains and grains pull-out from the Co binder phase can also be studied. Literature revealed that if the addition of Mo_2C content is more than 5 wt% then the exceptional differences in the microstructure of fracture surface is observed. Due to very refined grain the tendency of trans-granular failures decrease and inter-granular failures increase moderately, which increases the fracture toughness of the cermets. Also mean free path of binder (Co) increases causes to the more traces of tearing as shown in the **Fig.2.14** [7,9,13,48].

2.5.5 Comparison of Particle size with different secondary carbides

S. Kang *et al.* reported that The effect of secondary carbides (Mo_2C, NbC and TaC) in $(Ti_{0.93}W_{0.07})(C_{0.7}N_{0.3})$-20Ni cermets is shown in **Fig.2.15**. The addition of Mo_2C provides an average grain size of approximately **480** nm, while for the NbC and TaC additions, these values are approximately **680** nm and **640** nm, respectively.

It was studied that the dissolution of secondary carbide content in the Ni melt highly depends on its solubility and phase stability limit in Ni melt. WC and Mo_2C have low stability therefore dissolve more rapidly than the other stable carbides. The addition of Mo_2C results in considerably smaller particle size than other carbides [1,2,4,8-11,13,16].

Qian and Lim reported that The disappearance of Mo_2C during solid state sintering when the ratio of Mo_2C to Ni is less than or equal to 0.3 then most or even all the Mo_2C phases present in the Ti(C,N)-Mo_2C-Ni alloys can be dissolved in Ni after 1h at 1200 °C. However, when the ratio is greater than 0.3 then only partial dissolution of Mo_2C can be noticed even 10 h at 1200 °C [13].

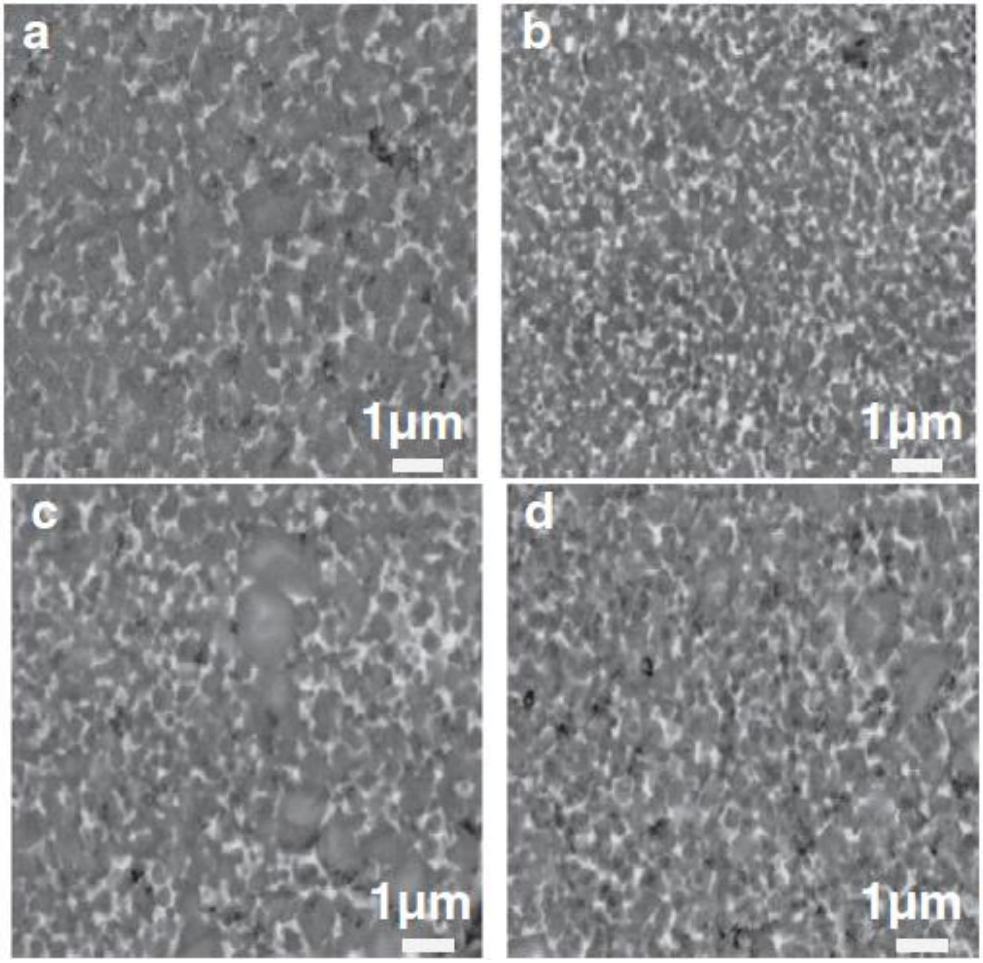

Fig. 2.15. SEM images of $(Ti_{0.93}W_{0.07})(C_{0.7}N_{0.3})$-8% MeC-20% Ni cermets (in wt.%): MeC= (a) none, (b) Mo_2C, (c) NbC, and (d) TaC.

2.6 Cermets sintered with different starting materials

Liu Y. *et al.* reported that an ultrafine cermet has different core-rim microstructure, ensuring in outstanding mechanical properties such as bending strength of 2210 MPa, Vickers hardness of 14.7 GPa and fracture toughness of 10.1MPa $m^{1/2}$. The small concentration gradient in core-rim structure and the vanishing of inner rims is beneficial to decrease in the residual stresses at the core-rim interface in (Ti, M)(C,N)-MxC cermets, and hence improvement in their fracture toughness [1,7,13].The resultant structures of cermets are completely different with different starting materials and maintaining the same total content of secondary carbides M,**Fig.2.16** [10,14].

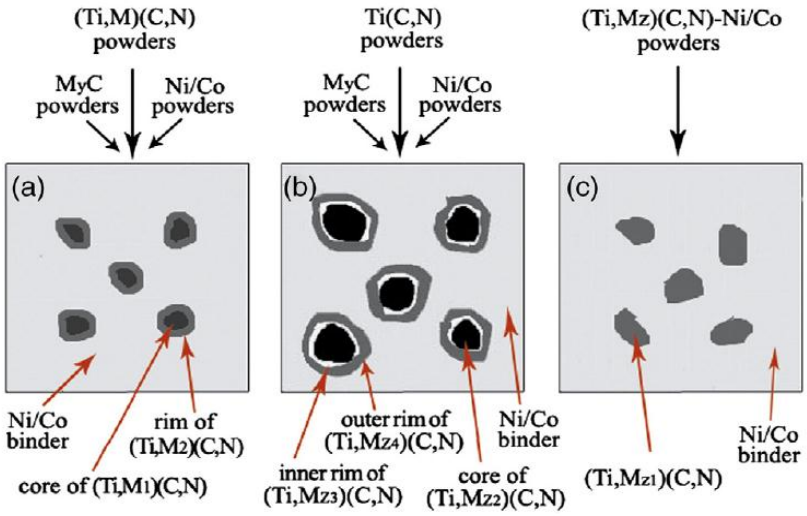

Fig. 2.16. Structural characteristics in (Ti, M)(C,N)-MxC (a),Ti(C,N)-MyC (b) and (Ti, Mz)(C,N) (c) cermets.

2.7 Metallurgical reactions during sintering

2.7.1 Reaction between nickel melt and TiCN

P. Ettmayer *et al.* reported that the pseudobinary eutectic points between TiC and Ni, or between Co and TiC, analogous eutectic points in Ni and TIN system or in Co and TiN system are either unknown or unpredictable by some researchers. Nitrogen-rich titanium carbo-nitride seperates from the binder melt, while TiC, Mo_2C and WC are dissolved in the binder melt according to their solubility limit. When Mo_2C and WC are present as elements in the as-recieved powder mixture, due to their high solubilities in the binder they are dissolved in the liquid phase accordingly. Hence, the liquid melt that outcomes during the initial stage of sintering is considerably rich in Mo or W, solubility of carbide/nitride are listed in **Table 2.3** [8].

Table 2.3. Solubility of carbide/nitride in different cermets system [8]

System	Co-TiC	Co-TiN	Co-VC	Co-NbC	Co-TaC	Co-Mo_2C	Co-WC	Ni-TiC	Ni-TiN	Ni-VC	Ni-NbC	Ni-TaC	Ni-Mo_2C	Ni-WC
Solubility of carbides/nitride (wt.%)	10	0.5	19	8.5	6.3	39	39	11	0.5	14	7	6.3	36	27

2.7.2 Degassing experiments

Ettmayer reported in his study that specially CO, CO_2, H_2O, H, and hydrocarbons, which are unrestrictly released during the heating up period. Therefore to avoid such possibilities of interrupting gases, the green pellets were heated up inductively in a quartz pipe. Therefore it is reduced to carbon mono oxide (CO). The contamination of oxygen in the powder mixture, probably as chemisorbed and begins to react. As temperature increases the rate of reaction increases slowly and it reaches maximum at 1100°C. If temperature increases further then the rate decreases, may be because of oxygen removal from the powder particles.

The rate of CO formation increases with increase in Nickel and cobalt and raise the shifting of the arm-wetting oxide layers on cemented carbide particles surface. The expansion of nitrogen gas started around 1200°C and reaches a peak at around 1300°C. After that increment in temperature cause decrease in rate of nitrogen degassing again and then constant shows in **Fig.2.17** [8].

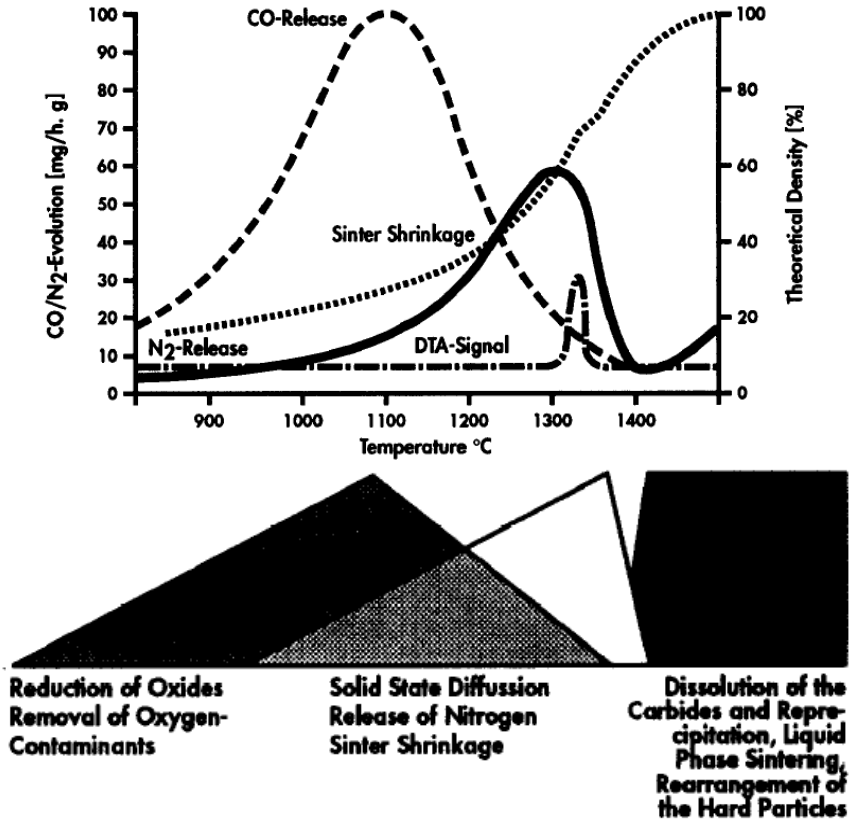

Fig. 2.17. The metallurgical reactions occurred during a sintering [8]

2.8 Preparation of ultrafine TiCN-based cermets

As per the Hall-Patch relation, materials with ultrafine grain have improved mechanical properties. It is reported in several publications that grain refinement will increase fracture toughness, bending strength and hardness of cermets. A incredible research have been done to consolidate ultrafine TiCN-based cermets to meet the cutting performance of the cermets [1,3,13].

2.8.1 Preparation of ultrafine/nano TiCN powder

For improving efficiency of cermets cutting tools, significant research studies conducted to develop TiCN-based cermets with ultrafine structures Four principle ways of preparing nano or ultrafine powders of TiCN are generally reported, namely self propagating reaction at high temperature synthesis, carbo-thermal reduction synthesis, and mechanically-induced self-sustaining reaction, chemosynthesis and ball-milling [1,3,13].

2.8.2 Carbo-thermal reduction synthesis

In this method generally TiO_2 and C powders are used as starting materials to prepare TiCN powder in N_2 at high temperature [1]. Carbo-thermal reduction method has been identified as a cheap method for powder preparation. [1,7,8,13].

2.8.3 SHS and MSR

It is an suitable method for synthesizing TiCN-based cermets using the pre-reacted hard components as the initial materials [1,14].

2.8.4 Chemosynthesis

In this process reaction temperature is lower and easy to control compare to the other preparation methods. It is reported in the literature that, TiCN powders can be prepared by polymer-to-ceramic transformation. But due to the complicated manufacturing process and high cost it is not used [1].

2.8.5 Ball-milling (Mechanical alloying)

Ball-milling is a type of grinder and it is used to grind the materials into fine powders. It is a process of formation of alloy phases by using mechanical energy from high energy ball mills which can be done by repeated cold welding, fracturing and re-

welding of powder particles. In recent times, it is one of the most popular non-equilibrium processing methods used in preparation of advanced materials. This technique can be used to metals, ceramics, polymers, and composite materials. Serious contaminations from the milling jar and balls during milling are also a limitation. Various types of ball-mills are available for milling, such as drum type ball mills, jet mills, bead mills, horizontal rotary ball mills, vibration ball mills and planetary ball mills. These mills differ in their capacity; speed of operation, and to control the operating temperature of milling. The proposed research aims to develop new ultrafine powder of TiCN by using high energy planetary ball-miller [1,32-36,43].

2.8.5.1 Planetary ball mills

Planetary Ball Mills (**Fig.2.18**) are used wherever the highest degree of particle size reduction is required. These mills are also used for colloidal grinding and give the energy input required for ball-milling. The very high centrifugal forces of a planetary ball mill result in very high pulverization energy in a less grinding times.

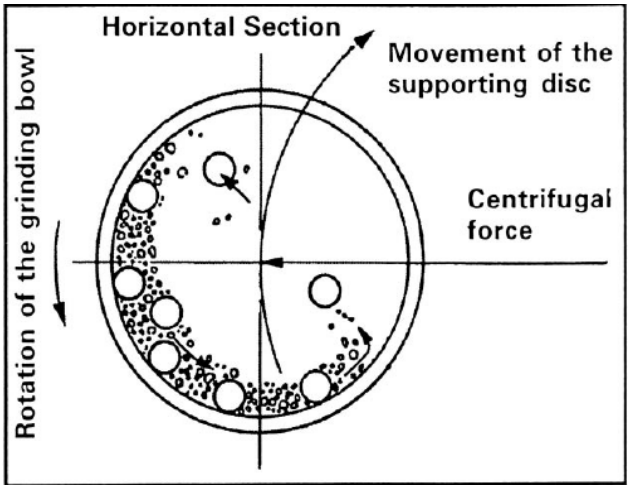

Fig. 2.18. Fritsch planetary ball miller [27]

Abrasion takes place when localized stresses are applied **(Fig.2.19a).** Cleavage of particle takes place when slow and relatively high intensity compressive stresses are applied which form particle size 50-80 % of the initial size of the particle **(Fig.2.19b).** Fracture takes palace when suddenly applications of intense impact stress then relatively smaller particle sizes with a comparatively bigger particle size **(Fig.2.19c).** [33]

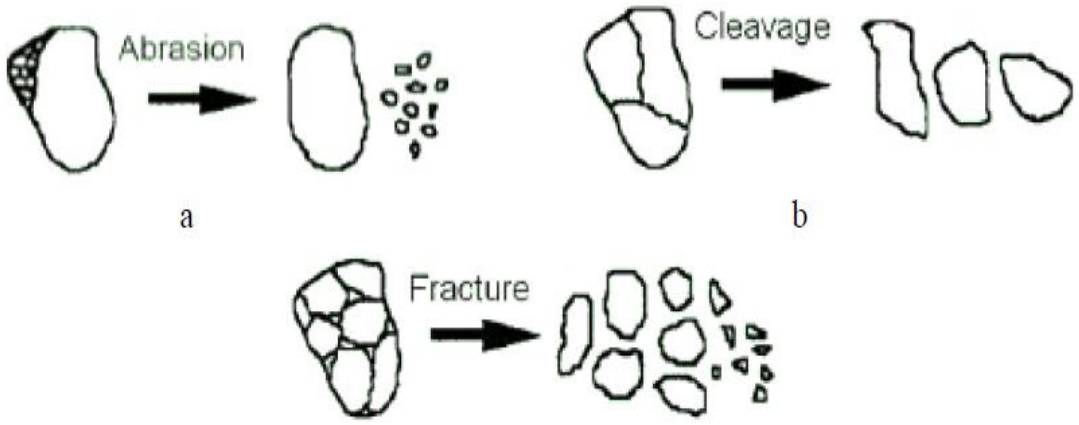

Fig. 2.19. Fragmentation mechanisms during ball milling [33]

2.8.5.2 Process parameters for ball-milling

There are various variables on which mechanical alloying depends and these variables have important influence in order to achieve desired reduced particles phase, microstructure, and properties. For a given starting composition of the powder, some of the important key variables that have an important influence on the final reduced phase of the milled powder are as follows-

2.8.5.2.1 Milling medium

The selection of grinding medium on basis of its size, nature, and size distribution is a significant step in order to achieve well ordered milling of materials. The selection of milling medium depends on the following factors.

2.8.5.2.2 Particle Size and hardness

The size of balls, used for grinding should be large in size relative to the size of powder particle to provide proper impact. Small size grinding balls are preferred to achieve fine milled powder. High difference in hardness of grinding balls and power offers very less contamination during milling. If the grinding balls have brittle nature then it will enhance the contamination of the milled powder due to chipping of its edges.

2.8.5.2.3 Milling speed

The higher rotation of milling jar provides higher energy into the powder due to higher kinetic energy at higher rotation of the mill. The maximum speed is determined by the design of mill jar which provides the specific limitation to mill jar in term of speed. The selection of speed for milling should be chosen properly to avoid the generation of temperature, phase decomposition.

2.8.5.2.4 Milling time

Milling time is one of the key parameter to reduce the size of the particle. It determines the breaking, fracturing and cold welding of milling powder. It should be selected properly to get steady state of the milling of the powder. The required duration will be fixed for each combination of parameters or given system of powders **Fig.2.20.**

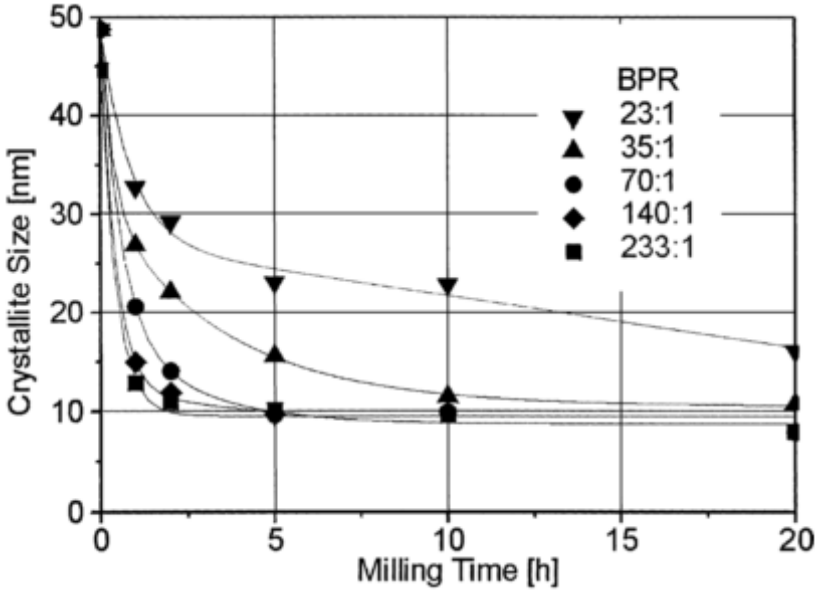

Fig. 2.20. Variation of crystallite size with milling time and ball-to-powder mass ratio [34]

2.8.5.2.5 Ball to powder weight ratio

The ball to powder weight ratio is one of key point during the milling process. Many researchers reported this ratio from low as 1:1 to high as 1000:1 for the milling. Ratio of 10:1 is most generally applied for small capacity ball milling.

2.9 Sintering of ultrafine/nano TiCN-based cermets

2.9.1 Spark plasma sintering (SPS)

Guillon *et al.* reported in his paper that field-assisted sintering technology (FAST) or spark plasma sintering is a pulsed direct current (DC) current activated, low voltage, and pressure-assisted sintering technique. SPS is a newly developed rapid consolidation technique by which sintering is possible at low temperatures and short duration as compare to the conventional sintering. It involves heating of powder particles with electrical energy and effectively applying high temperature spark plasma **(Fig. 2.21**) [23,24].

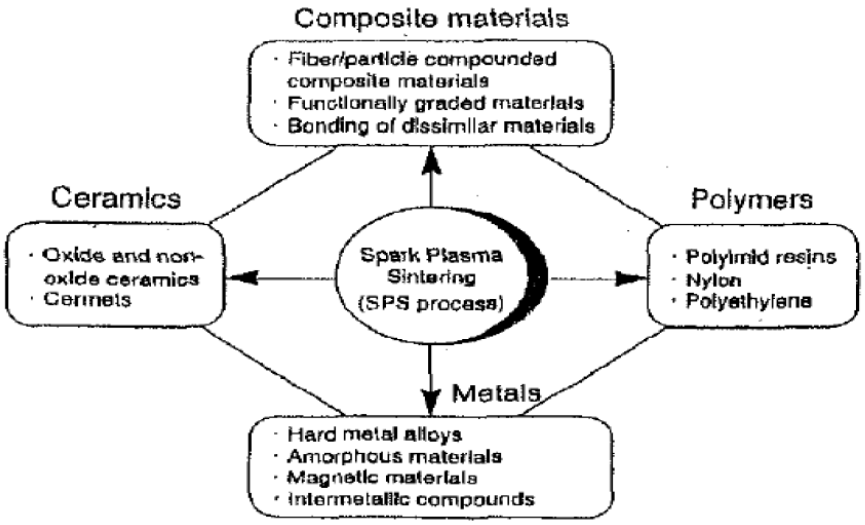

Fig. 2.21. Flow chart of materials covered by SPS processing

2.9.1.1 Principle of the SPS

The principle of SPS is electrical spark discharge technique in which plasma is generated by low voltage pulsed current at a point momentarily. It can easily consolidate a high-quality, homogeneous sintered compact due to uniform localized heating.

2.9.1.2 DC pulse current energizing effect

The ON-OFF DC pulse energizing effect produces- (1) spark plasma, (2) spark impact pressure, (3) Joule heating, and (4) an electrical field diffusion effect. Advancing sintering in these processes are the Joule heat generated by the power supply (I^2R) and the plastic flow of material takes place by the applied pressure. The SPS is an electrical sintering process which applies an ON-OFF DC pulse voltage and current (**Fig.2.22).**

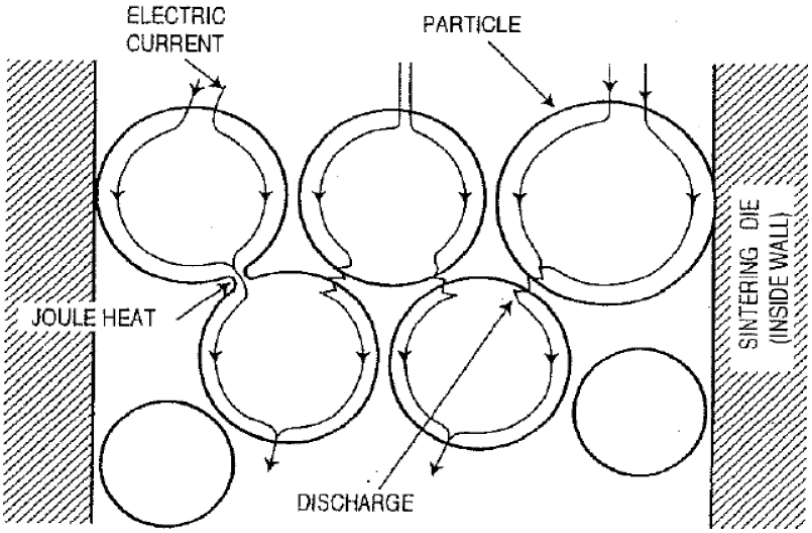

Fig. 2.22.. Pulsed current flow through powder particles

2.9.1.3 Mechanism of processing

Localized heating is generated momentarily if spark takes place between the powder particles. Such high temperature cause evaporation and melting on the powder particles surface followed by "neck" formation after that neck growth takes place. **Fig.2.23** and **Fig.2.24**.

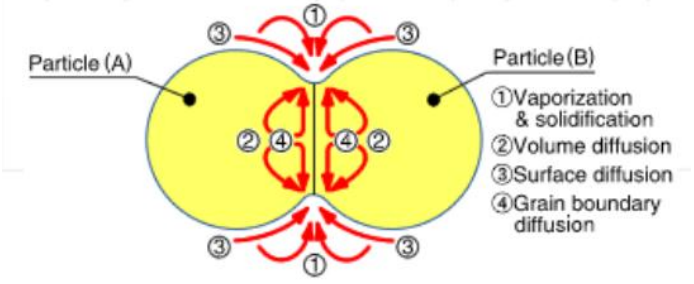

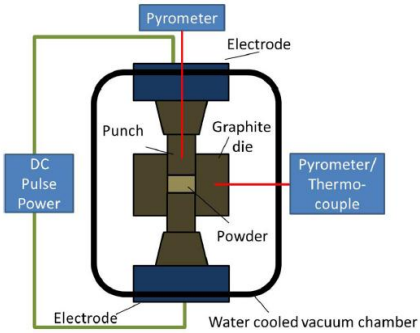

Fig. 2.23. Diffusion path during sintering Fig. 2.24. Working diagram of a FAST

2.9.1.4 Process parameter of SPS

Munir *et al*. reported that there are several process parameters on which desired properties of the sintered sample depends. These parameters need to be optimized to get better densification, microstructure and other mechanical properties. Some important sintering parameters which have significant influence on properties of product are discussed below [20].

2.9.1.4.1 Effect of heating rate

The effect of heating rate has been studied considerably in both pressure less and pressure assisted sintering. In pressure less sintering, higher heating rates increase densification by by-passing the reaction occurring via non-dandifying mechanism of surface diffusion and by providing an auxiliary driving force to overcome the large thermal gradients.

2.9.1.4.2 Effect of pressure

Pressure is applied to attain higher densification at same temperature. The mechanical pressure is applied for the particle rearrangement during sintering and breaking of agglomerates in case of nano powders. The significance of pressure is also depends on particle size of powder.

2.9.1.4.3 Effect of current

The effect of current in SPS is like function of brain in the human being. Due to current joule heating takes place at a point which cause diffusion of atoms and therefore densification is achieved. Current also have effect on mass transport. The influence can be demonstrated through the electron wind effect.

2.10 Advantage of SPS over Convectional sintering

SPS provide number of advantages over conventional sintering. In SPS heating takes place directly at powder particles but in the convectional sintering powder is hated by radiation from furnace wall. Due to fast processing grain growth can be restricted. In SPS the plasma pressure (sputtering pressure) helps to remove adsorptive gases from the powder surface.

2.11 Spark Plasma Sintering of TiCN-based Cermets

Angerer *et al*. reported that spark plasma sintering of nano titanium carbo-nitride powders have been conducted in the temperature range 1600°C -1800°C with soaking time 1 min. study showed that density of SPS samples achieved over 95%, which is considerably greater than that obtained by pressure less sintering, gas pressure sintering(GPS) and hot pressing. GPS sintered samples have approximately same density

(~95%), but higher temperature is required as 2100°C and holding time of 45 min. Also the GPS sintered sample have grain size about three times that of SPS samples [25,42].

O.Z. Lozynskyy *et al* reported that synthesis of commercially obtainable nano structured titanium carbo-nitride powder can be conducted by SPS at 1300 - 1600°C. The influence of multi stage (non-linear) heating and loading regimes on synthesis of high melting point has been discovered. SPS prepared TiCN material has achieved fully dense and finer microstructure having average grains size of 150nm [26,46].

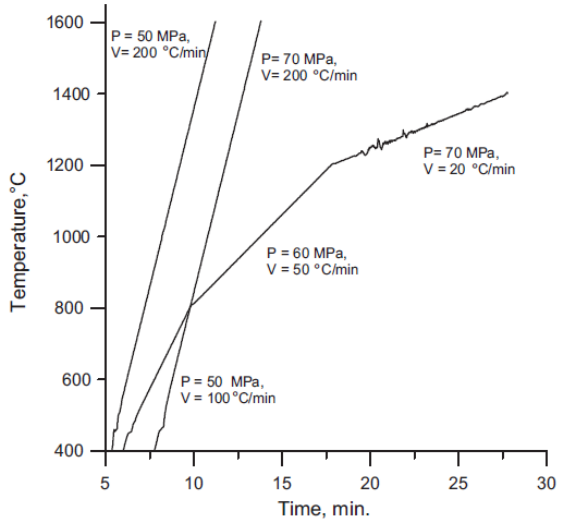

Fig. 2.25. Single and multiple stage regimes of SPS

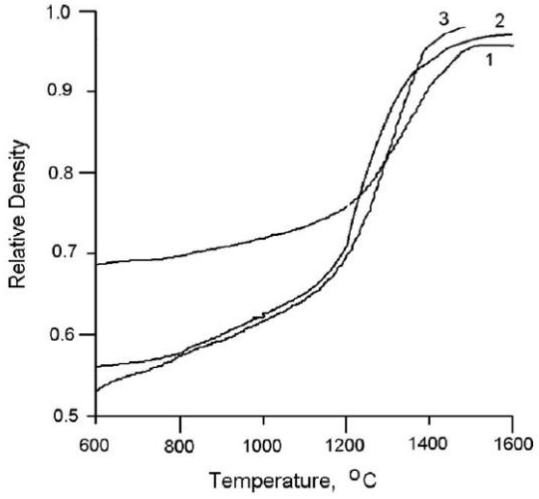

Fig. 2.26. Relative density as a function of sintering temperature: (1) Single (2) Single (3) Multi stages

In case of one stage regime (P=50MPa and 70MPa load, heating rate 200°C/min, T_{max} = 1600°C without soak), and another one was a multi stage regime with systematic increase of pressure from 50-70MPa and simultaneously decrease of heating rate from 100°C/min to 20°C/min as shown in the **Fig.2.25** and **Fig.2.26** .

2.12 Tribological characteristics of TiCN-based cermets

Cermets wear characteristic is a strong function of microstructure, grain size and shape, grain boundary toughness, and the operating conditions [37]. As the high temperature strength and hardness is concerned then it is important to describe the wear phenomenon and performance of TiCN-based cermets. Generally, during high speed cutting with TiCN-based cermets, following types of wear are observed fretting wear, sliding wear, erosive wear, crater wear and creep wear [1]. TiC-based cermets have advantage over WC-base hard metals as the wear performance is concerned because they have lower coefficient of friction and higher oxidation resistance [36].

2.12.1 Fretting wear

Fretting wear is the wear process in which the removal of material takes place from two contacting surfaces because of friction due to small relative motion. It was found that during fretting wear, firstly wear is due to abrasive mechanism and then due to heat of friction. During the course of wear a Ti-rich oxide tribo-layer is formed. Sometimes, the oxide layer formed containing different secondary carbides **(Table. 2.4) [1]**.

Table. 2.5. Friction and fretting wear rate, as-studied TiCN-based cermets [1]

Compositions	**Steady-state COF**	**Wear rate of cermets (×10−6 mm^3/Nm)**	**Wear rate of steel ball (×10−6 mm^3/Nm)**
TiCN–20Ni	0.46	3.0	7.1
TiCN–20Ni–10WC	0.46	5.0	14.1
TiCN–20Ni–10NbC	0.46	5.2	16.9
TiCN–20Ni–10TaC	0.43	3.5	12.4
TiCN–20Ni–10HfC	0.43	3.8	6.5

U. Persson et al reported that the level of adhesion can be leveled by using the largest adhesion force. Both coating and the base material during fretting wear were affected. Therefore TiN coating decreases the chance of adhesive wear for various materials [38].

P.Q. Campbell found in his study that during fretting wear experiments with the Cr-steel counter-bodies, all the ceramics and cermets have a steady state COF between 0.6 to 0.7, except TiCN-based cermets [39].

2.12.2 Crater wear

For longer life of cutting tools, As reported in the literature that addition of WC into TiCN–20Ni cermets (≤10 wt.%) was advantageous to enhance the wear performance of the cermets [1].

Kumar BVM et al investigated that the capacity of TiCN-20wt.% Ni-(0-15wt.%)WC cermets under orthogonal cutting conditions, as cutting speed and feed rate increases then steady state cutting achieved with lesser cutting force. The optimum content of WC addition in TiCN–20Ni cermets was beneficial up to 10 wt.%. In case of cermets tribo-chemical wear and abrasion are the general crater wear mechanism of the studied cermets. If the WC content in the cermets increases then the tendency of mechanical abrasion and grain pull-outs increases [28].

2.12.3 Creep wear

As for as the high speed cutting performance of cermets at elevated temperature is concerned therefore it is very important to study about mechanisms operating at elevated temperature.

It is reported in the literature that while high speed cutting operation at elevated temperature, mainly there are three mechanisms which causing the deformation: brittle, tough with limited plasticity and creep performance. Carbon controls both the two deformation mechanisms by the self diffusion in the TiCN phase [1].

2.12.4 Erosion wear

Erosion of cermets have been defined by the combination of plastic deformation in the impact zone followed by growth of lateral cracks. It was studied that the composition of TiCN based cermets certainly plays key roles in the erosive wear resistance [1]. According to the relation-

$$E=C*K^{m}_{IC}*H^{n}v \qquad \text{.....(4)}$$

Where E is the erosion rate,

C is proportionality constant;

K_{IC} and Hv are the fracture toughness and Vickers hardness of the prepared materials; and m and n are constants.

Vijh A.K. reported that the coefficient of friction is directly related to the values of the bond energies metals, hardness and abrasive wear inversely proportional to the magnitudes of self-adhesion [30]. Abrasive-erosion (two-body abrasion) rate of TiC-Ni-Mo-based cermets is highly depends on the ratio of Ni:Mo binder composition and also on wear conditions at ambient temperature **Fig.2.27** [36].

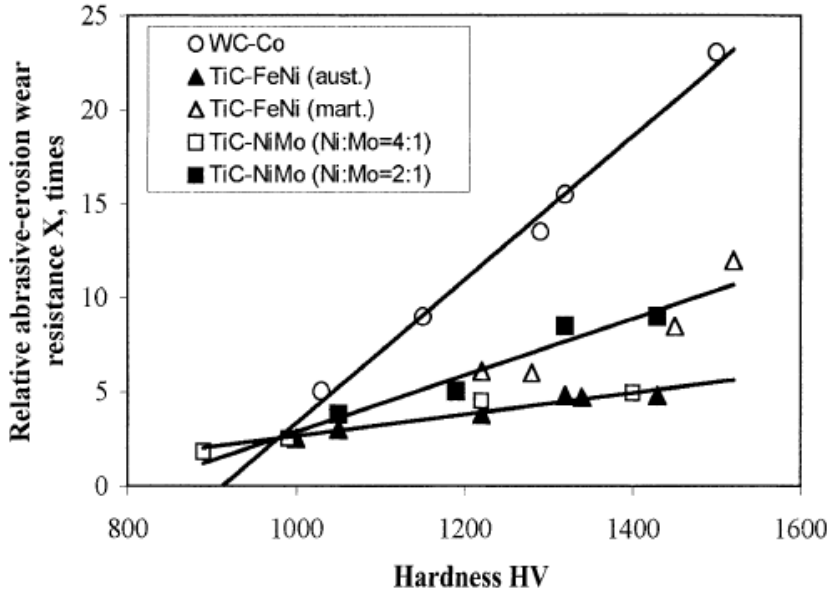

Fig. 2.27. Abrasive-erosion wear resistance *X* of TiC-Ni-Mo and TiC-FeN cermets and WC cemented carbides vs. hardness number [36]

Literature review indicates that the cermets composition can be designed to restrict coarsening of crystallites in order to improve mechanical and wear properties of TiCN-based cermets. Mo_2C addition is expected to restrict coarsening by enhanced dissolution during sintering, while WC improves densification.

However, the effect of Mo_2C addition on microstructure and mechanical characteristics of TiCN-WC-Ni-Co cermets is not thoroughly investigated probably because of the processing difficulties. The performance of such novel cermets in high temperature erosion behavior is not known.

Therefore, the present investigation is aimed to prepare ultrafine TiCN-based cermets via rapid sintering technique, spark plasma sintering, and study their performance in high temperature erosion wear conditions. Microstructural and mechanical features will be correlated with mechanism of material removal.

In this Chapter, experimental procedure involved in preparation and wear performance of TiCN-10wt%WC-10wt%Mo_2C-10wt%Ni-10wt%Co cermets is explained. First, details about milling/mixing of powders and spark plasma sintering of powder mixtures are given. The characterization involved in each stage of mixing is explained. This is followed by details of phase analysis, microstructural characterization and mechanical property evaluation of sintered cermets. Finally, test procedure to evaluate the performance of the developed cermets in erosion wear conditions is described.

3.1 Material preparation

TiCN (99.8% purity, <5 μm avg. particle size), Mo_2C (99% purity, 5-10 μm avg. particle size), WC (99% purity, < 800nm avg. particle size), Ni (99.5% purity, < 1μm avg. particle size), Co (99.5% purity, < 1μm avg. particle size) powders were used as starting materials. SEM images of as-received powders are shown in **Fig.3.1**.

The composition is selected on the basis of the literature findings that the 10 wt% WC addition is required for proper densification and good combination of mechanical or wear properties [31]. A 20 wt% binder is recommended to maintain decent toughness [5]. Equal amounts of nickel and cobalt are selected to maintain good wettability of liquid melt with the ceramic particles and restrict coarsening during sintering [5]. Thus, the cermets composition of 60wt%TiCN-10wt%Mo_2C -10wt%WC-10wt%Ni-10wt%Co is selected for the present work.

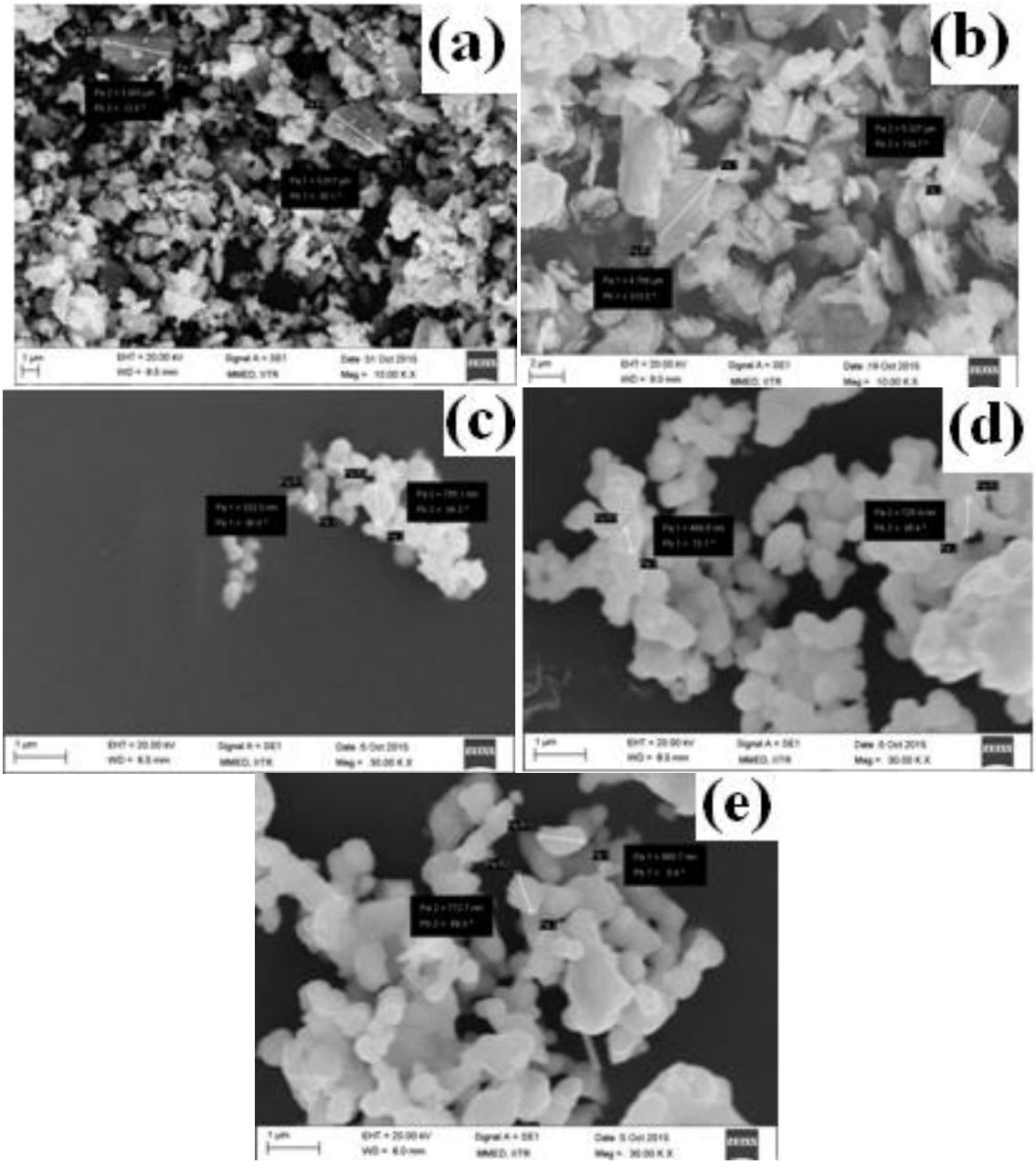

Fig. 3.1. SEM images of as-received powders and their average particle size -(a) TiCN < 5µm (b) Mo_2C 5-10µm (c) WC< 800nm (d) Ni <1µm and (e) Co <1µm

3.2 Ball milling

First of all, as-received TiCN (<5µm avg. particle size), and Mo_2C (5-10µm avg. particle size) powders were ball milled for the period of 70 h and 30 h, respectively in a high energy planetary ball mill (Fritsch PM100). Tungsten carbide balls were mixed with respective powders at a ball-to-powder weight ratio of 10:1. A tungsten carbide jar was used and all the milling was governed at a speed of 300 rpm in toluene atmosphere. The

mixed slurry was dried in an oven at a temperature of 100°C for 1 hour and the dried powder mixture was crushed in a mottle & pestle to remove the agglomerates of the powder and then sieved through No.450 fine mesh. The milled and mixed powders were studied for the phase evolution using a X-ray diffractormeter (XRD D8 Discover, Rigaku).

3.3 Spark plasma sintering

The powder mixtures were sintered in a spark plasma sintering furnace (SPS-625, Fuji Electronics Ltd., Japan) at 1250-1300°C and 40-50 MPa for 3- 5 min for optimizing the sintering parameters. SPS is a newly developed rapid consolidation process which makes possible sintering and sinter-bonding at the low temperatures and short interval of time as compare to the conventional sintering. A typical spark plasma sintering machine is shown in **Fig.3.2**.

Fig. 3.2. Spark Plasma Sintering Machine

After the sintering, the samples were removed by hydraulic press and graphite layer was removed from the surface of the sample by using belt polishing. After

removing the graphite layer sintered sample was polished on auto polisher by using diamond suspension. Firstly sample was polished on 45µm plate for 25-30 min. After that the sample was polished on 15µm, 6µm, 1µm plate and finally up to 0.05µm plate, (in **Fig.3.3)**.

Fig. 3.3. (a) Belt Polishing Machine (b) Auto Polisher

3.4 Density measurement

The density of the sintered composites was measured by Archimedes principle. For calculating theoretical densities by rule of mixtures, theoretical densities (gm/cc) of as received powders considered.

$$\frac{1}{\rho} = \frac{x_{TiCN}}{d_{TiCN}} + \frac{x_{WC}}{d_{WC}} + \frac{x_{Mo2C}}{d_{Mo2C}} + \frac{x_{Ni}}{d_{Ni}} + \frac{x_{Co}}{d_{Co}} \quad \ldots\ldots\ldots(3.1)$$

ρ= Theoretical density powder mixture

x_{TiCN}, x_{WC}, x_{Mo2C}, x_{Ni} and x_{Co} = Weight percentage of respective powders.

d_{TiCN}, d_{WC}, d_{Mo2C}, d_{Ni} and d_{Co} = Density of respective powders.

3.5 Micro hardness analysis

The micro hardness of the polished sample was calculated by Vickers indentation (Leica, VMHT (MOT), Germany) at a 20 N load for a dwell time of 15s. All the readings of hardness were taken at different locations at same load of 20 N. Normally the average

of 10 readings of hardness is reported. The instrument which is used to measure the hardness is shown in **Fig. 3.4.**

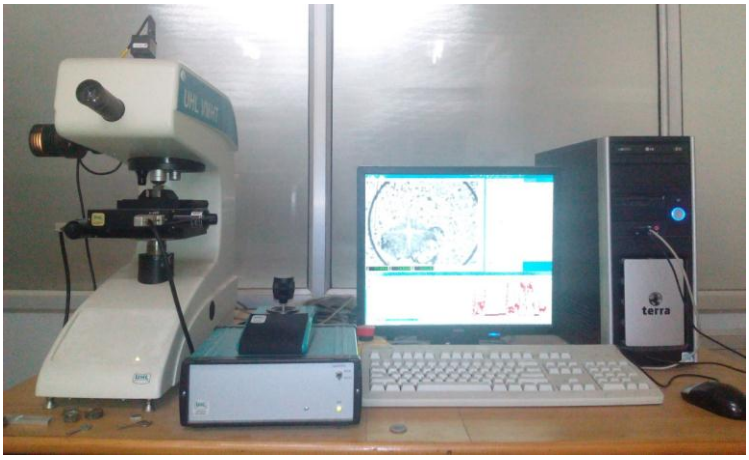

Fig. 3.4. Vickers Micro-hardness tester

3.6 Fracture toughness

Fig.3.5 shows the Lengths of crack generated by Vickers's indentation(AVK-C2, Akashi Corporation, Japan) at a 20 N load for 15s were measured and fracture toughness (K_{IC}) in MPa*m½ was calculated by using this relation-

$$KIc = 0.016 * \left(\frac{E}{H}\right)^{1/2} * \frac{P}{c^{3/2}} \qquad \text{.....(3.2)}$$

Where, c = (L/2) + a

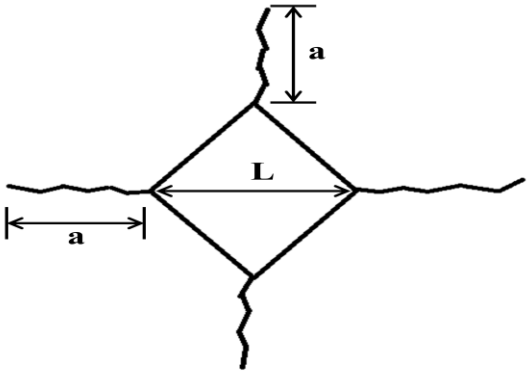

Fig. 3.5. Crack generated by Vickers indentation

Where, L= Length of the diagonal of the indentation,

P is applied load (N),

c is crack length (m),

H is hardness (GPa) and E is elastic modulus of composite (GPa),

This is estimated by rule of mixture using elastic modulii of all the elements.

3.7 High Temperature Erosion Tester

Erosion test was performed using high temperature erosion testing machine (in **Fig.3.6**). Silicon carbide erodent particles 45-75μm in size was dried in an oven at 100°C for 1 h and was mixed with air. The mixed air jet passed through nozzle of 1.5 mm diameter and were subjected to eroded the polished surface of the composite at a stand-off distance of 10 mm. Air pressure was controlled to maintain the particle velocity at 50 m/s with a flow rate of 3 g/min. Erosion tests was performed at an impingement angles of 90° for 15 min. at Room Temperature and at elevated temperature (400°C).

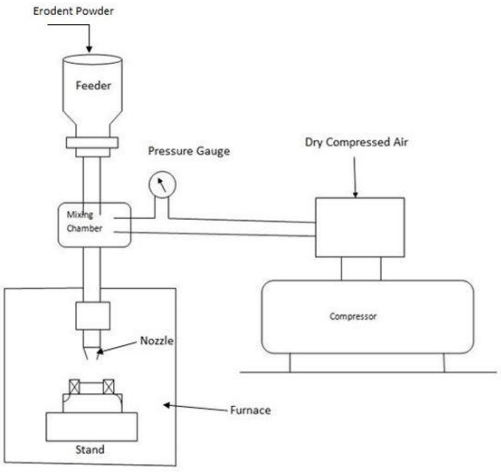

Fig. 3.6. Schematic diagram of high temperature erosion tester

The weight loss of the sintered ceramics was measured to an accuracy of ±0.1 mg. The average weight loss in steady state was converted to average volume loss and steady state erosion rate E in mm^3/kg was determined using the following formula.

$$E = \frac{V}{M} \qquad \text{.....(3.3)}$$

Where V is volume of the material removed in steady state in mm^3 and M is the mass of erodent particles used in steady state in kg. The erosion results were checked for the reproducibility by conducting whole experiment at least twice for each composition and angle of impingement. Material removal mechanisms were elucidated using SEM-energy dispersive spectroscopy (EDS) analysis of eroded surfaces.

Table 3.1. Experimental parameters for high temperature erosion test

Erodent material	**Erodent particle size**	**Impact velocity**	**Temperature**	**Impact angle**	**Discharge rate**	**Test duration**
Silicon carbide	45-75µm	50m/s	RT and (400°C)	90°	3 g/min	15min

Results obtained from ball milling, mixing of powders are explained. Density results obtained after spark plasma sintering are given. The microstructural features, phase analysis of sintered mechanical properties of sintered cermets are described. This is followed by results obtained from erosion test. The eroded surfaces are studied for the wear mechanisms.

4.1 Powder milling

Typical images of powders obtained through milling of TiCN powders and Mo_2C powders are provided in **Figs. 4.1 and 4.2.**, respectively. The average particle size reduced with increase in milling time and the average particle size obtained after milling of TiCN powders for 70 h is less than 100nm and for Mo_2C powders it is 300 nm in 30 h.

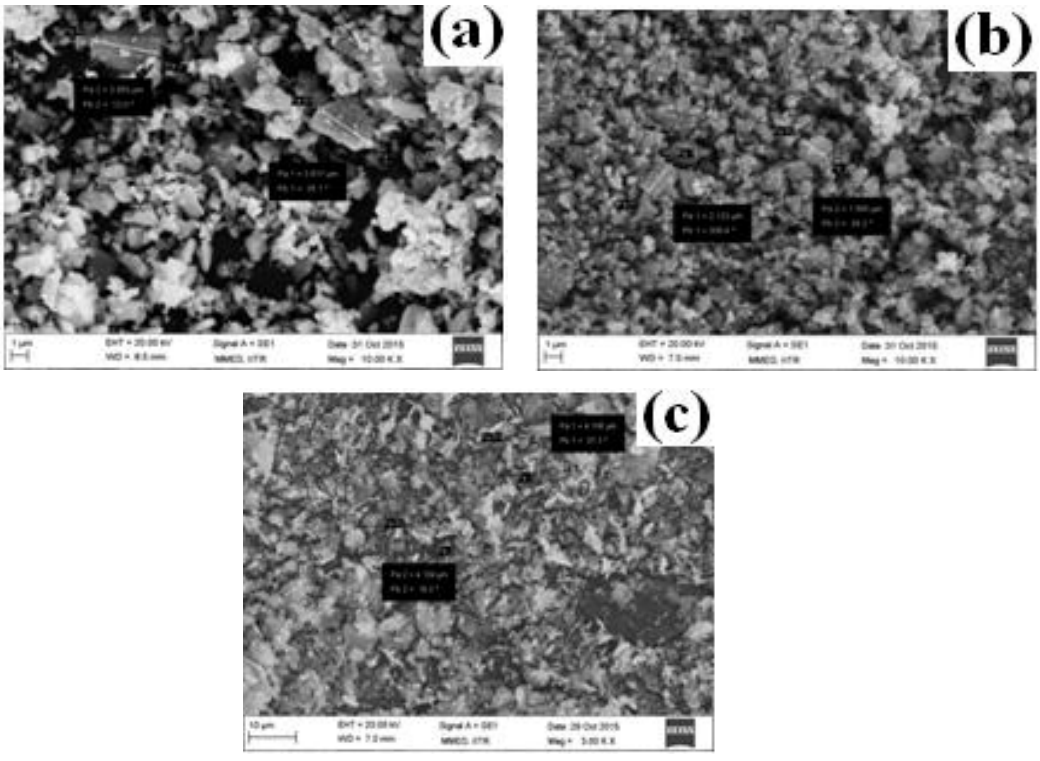

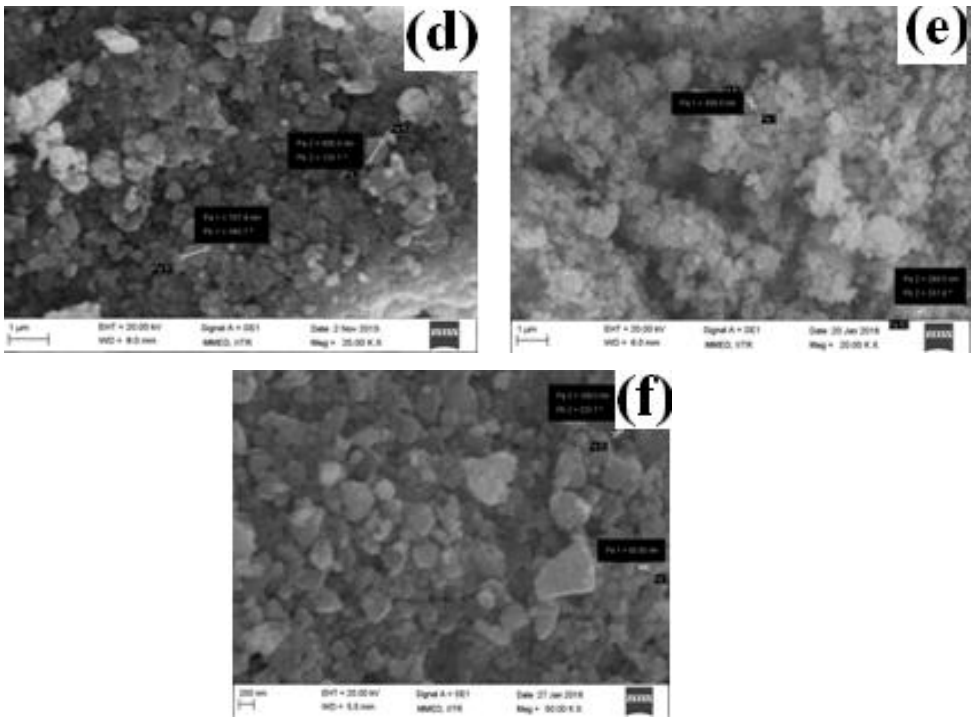

Fig. 4.1. SEM images of ball-milled TiCN powder and average particle size -(a) <3µm after 5h (b) <2µm after 10h (c) <1µm after 20h (d) <600nm after 40h (e) <300nm after 60h (f) <100nm after 70h

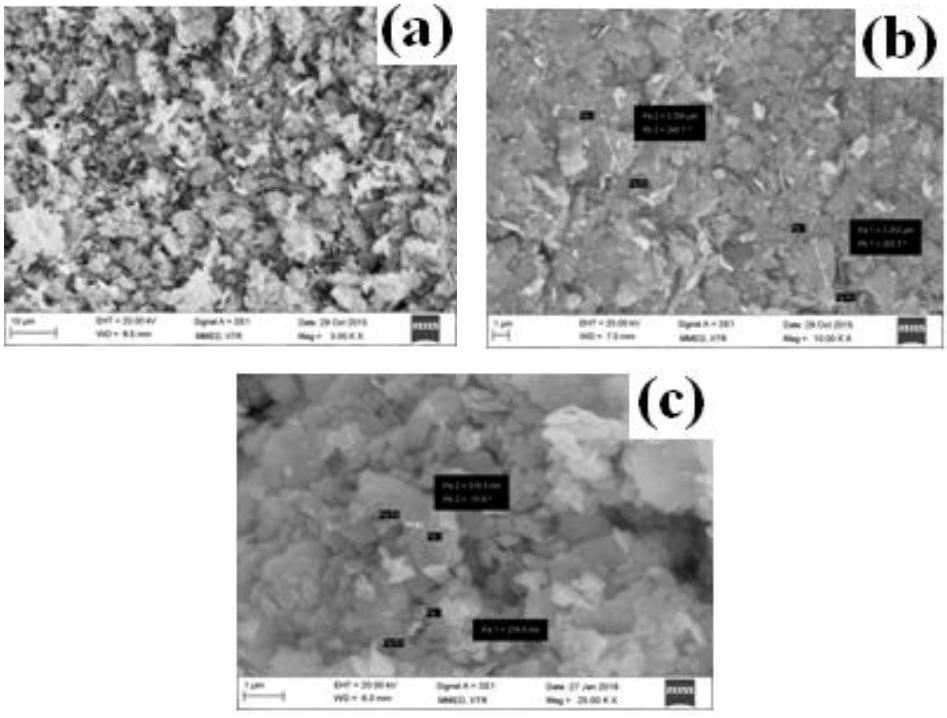

Fig. 4.2. SEM image of ball-milled Mo_2C powder (a) <5µm after 5h (b) < 3 µm after 15h (c) < 300nm after 30h

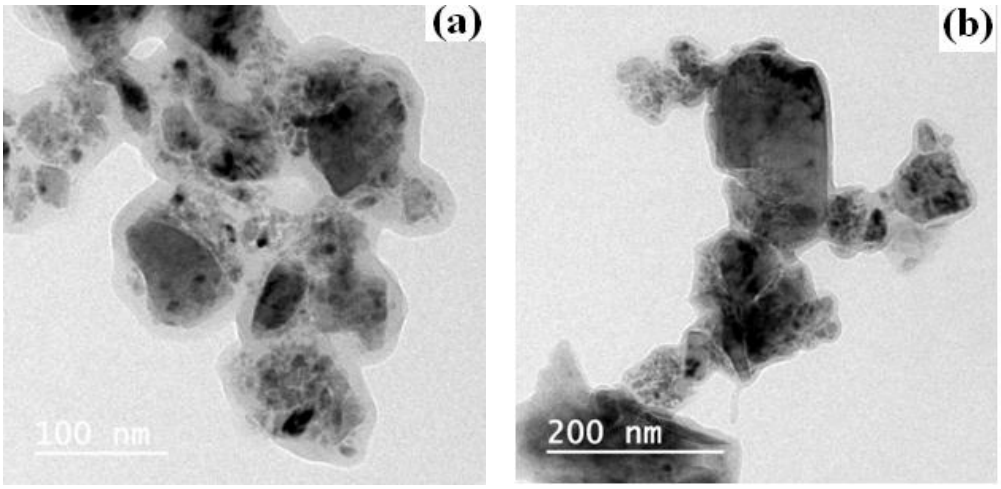

Fig. 4.3. TEM image of oxide-layer formed after 70h milled TiCN powder

Further, the transmission electron microscope (TEM) analysis confirms the nano sized powders and indicate the agglomeration (in **Fig. 4.3**). Also, the thin oxide layer enveloping the powder particles can be noted. The milled powders of TiCN and Mo_2C were mixed with WC, Ni and Co in the appropriate proportions and mixture was mixed for 8 h, 48 h and 72 h to obtain uniform mixing. SEM images and corresponding EDS and X-ray mapping analysis for the powder mixtures are shown in **Fig. 4.4- 4.6**. X-ray mapping analysis reveals increased uniformity in mixing after 72 h. EDS analysis indicated increased oxygen content with increase in mixing time.

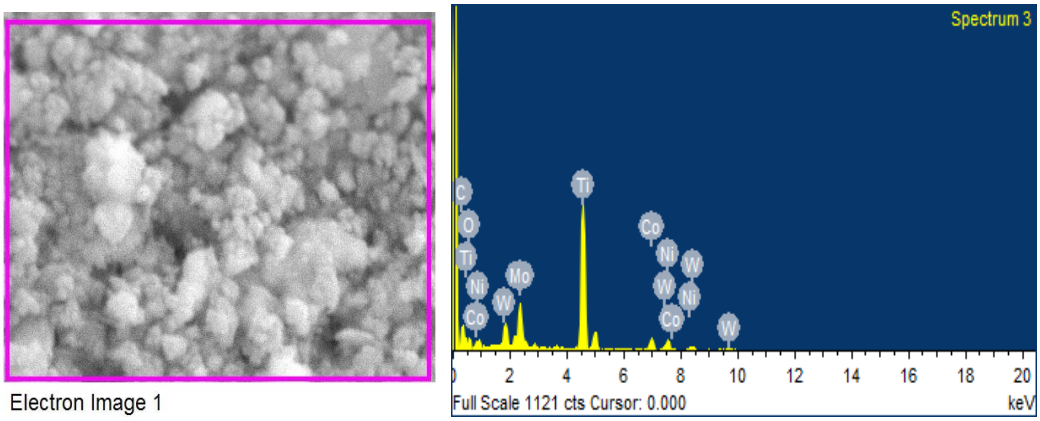

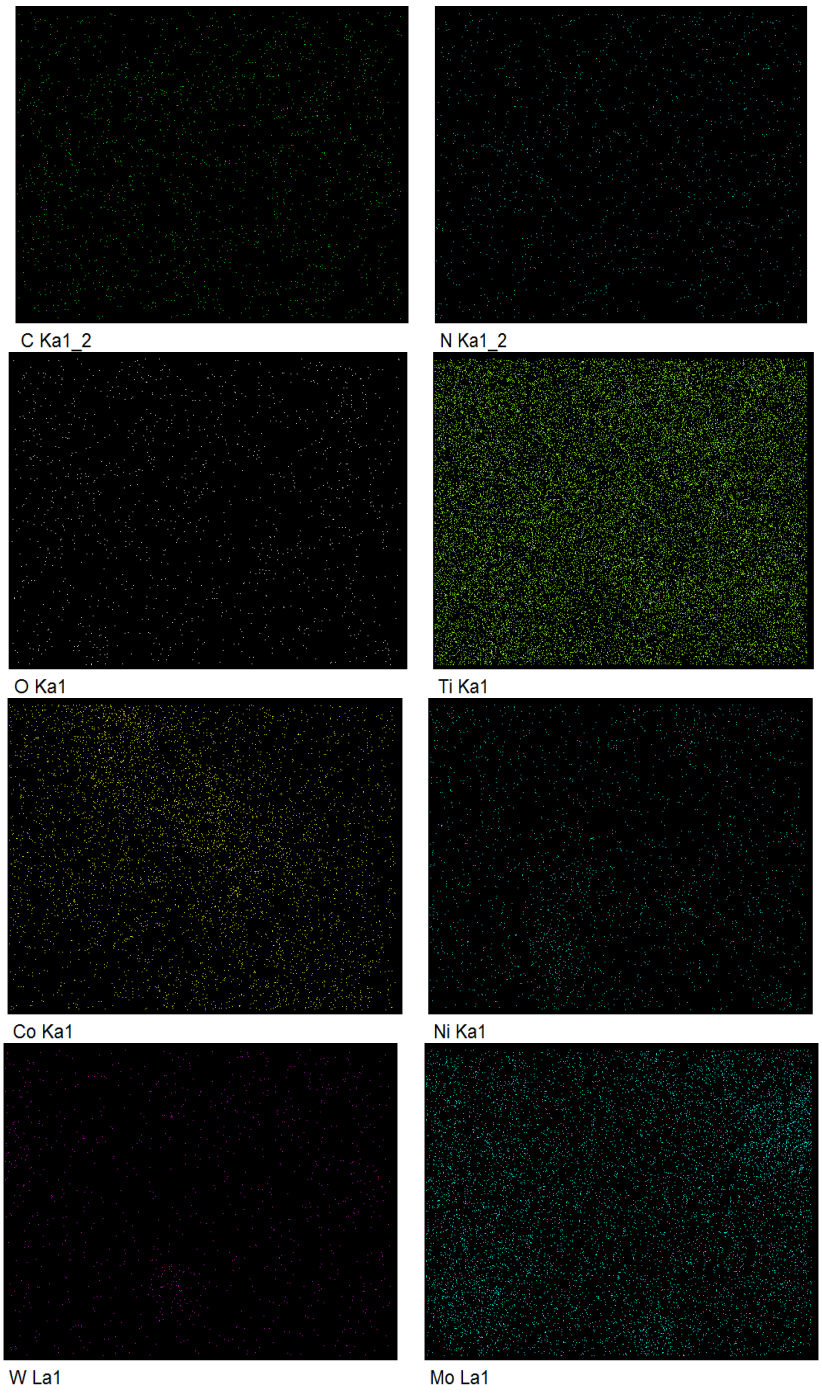

Fig. 4.4. EDS analysis of 8 h powder mixture of TiCN with 10wt% Mo_2C-10wt% WC-10wt% Ni-10wt% Co.

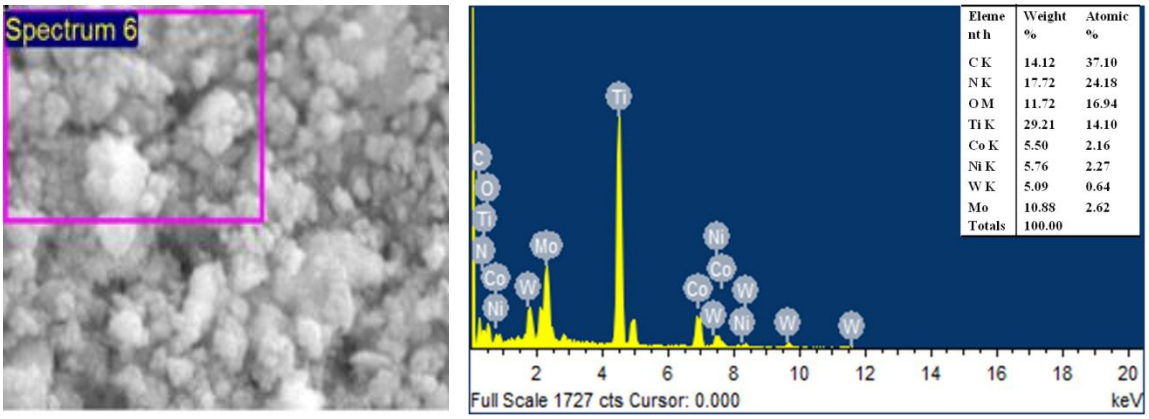

Fig. 4.5. EDS analysis of 48 h powder mixture of TiCN with 10wt% Mo_2C-10wt% WC-10wt% Ni-10wt% Co.

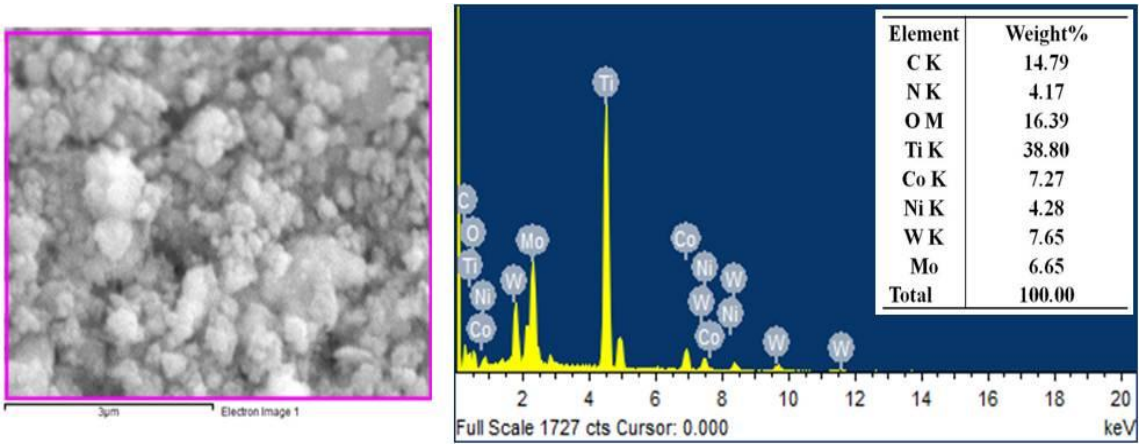

Fig. 4.6. EDS analysis of 72 h powder mixture of TiCN with 10wt% Mo_2C-10wt% WC-10wt% Ni-10wt% Co.

XRD analysis of as-received powders, ball milled powders and powders mixture are shown in Fig. 4.7.to 4.9. XRD analysis reveals no other phase. It is possible that the peak intensity of any other minor phases is out of the detection limit of the XRD instrument. Intensity of peaks decreased due to the peak broadening and also noise increased due to successive milling.

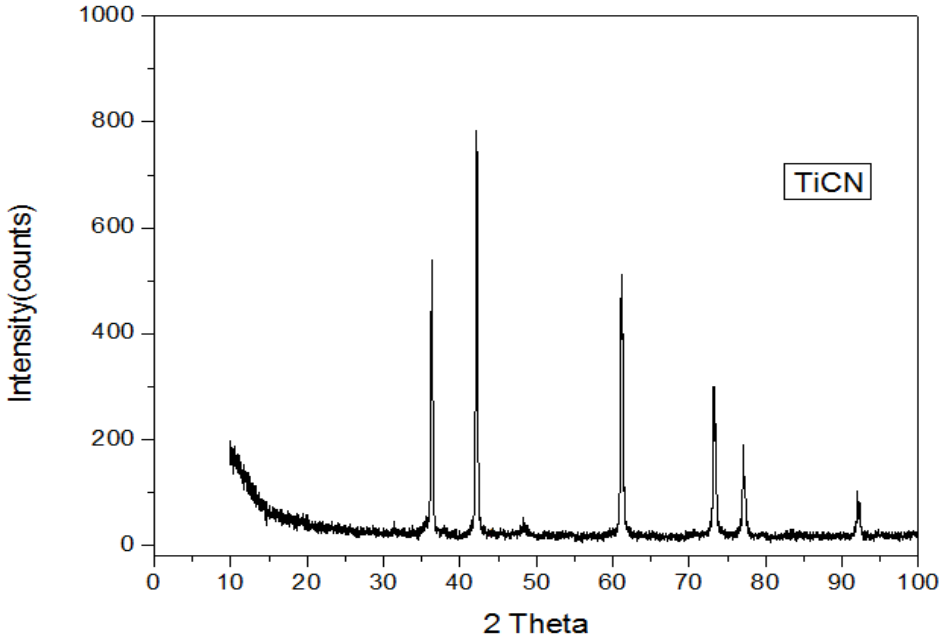
TiCN
Intensity(counts)
2 Theta
0
200
400
600
800
1000
0
10
20
30
40
50
60
70
80
90
100

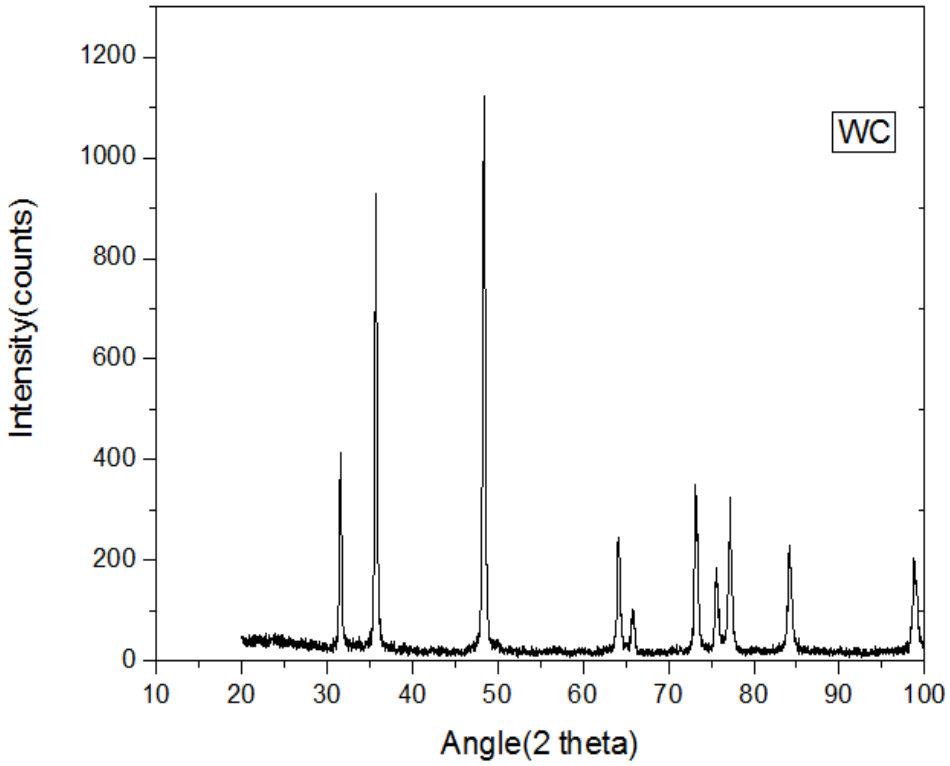
WC
Intensity(counts)
Angle(2 theta)
0
200
400
600
800
1000
1200
10
20
30
40
50
60
70
80
90
100

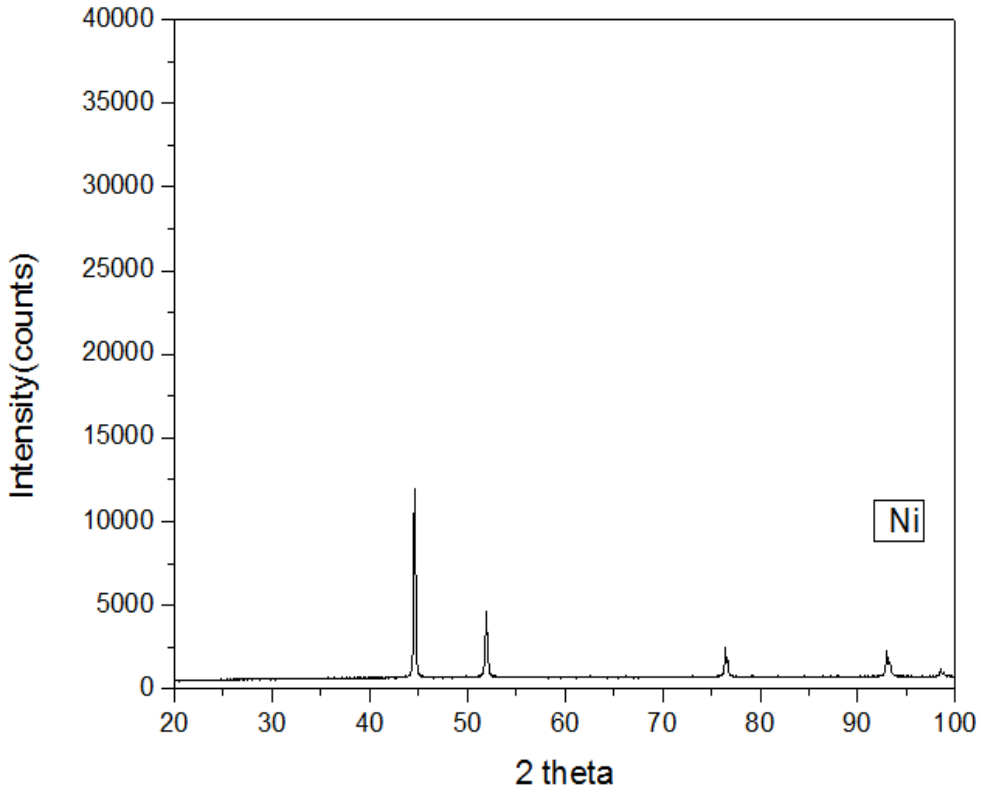
Intensity(counts)
2 theta
Ni

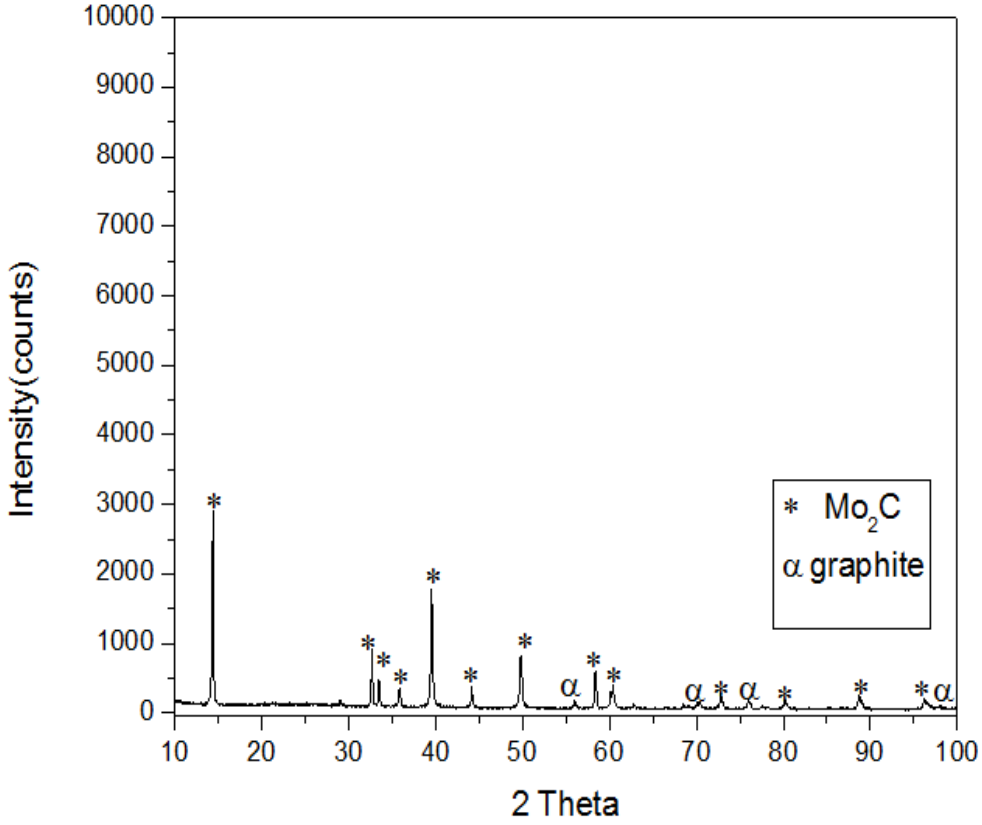
Intensity(counts)
2 Theta
* Mo2C
α graphite

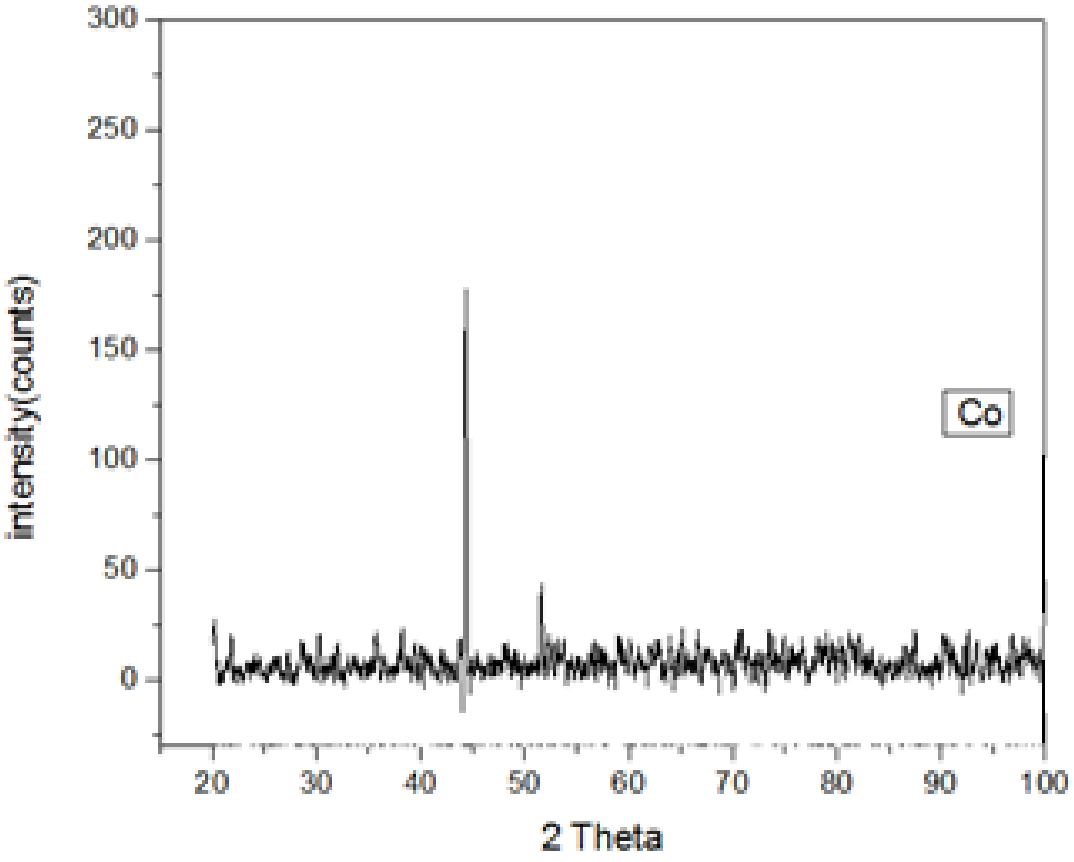

Fig. 4.7. XRD pattern of as-received powders

X-ray powder diffraction (**XRD**) is a rapid analytical technique primarily used for phase identification of a crystalline material and can provide information on unit cell dimensions. The **analyzed** material is finely ground, homogenized, and average bulk composition is determined. some oxide peaks are present after successive milling and mixing. It is possible that excessive milling caused contamination of WC from balls or vial of the mill, which is oxidized to WO. The oxidation of binder phase can also be noted from the XRD analysis of powder mixture. The XRD analysis of powder mixture for 8h, 48h and 72h respectively is shown in **fig.4.9**.

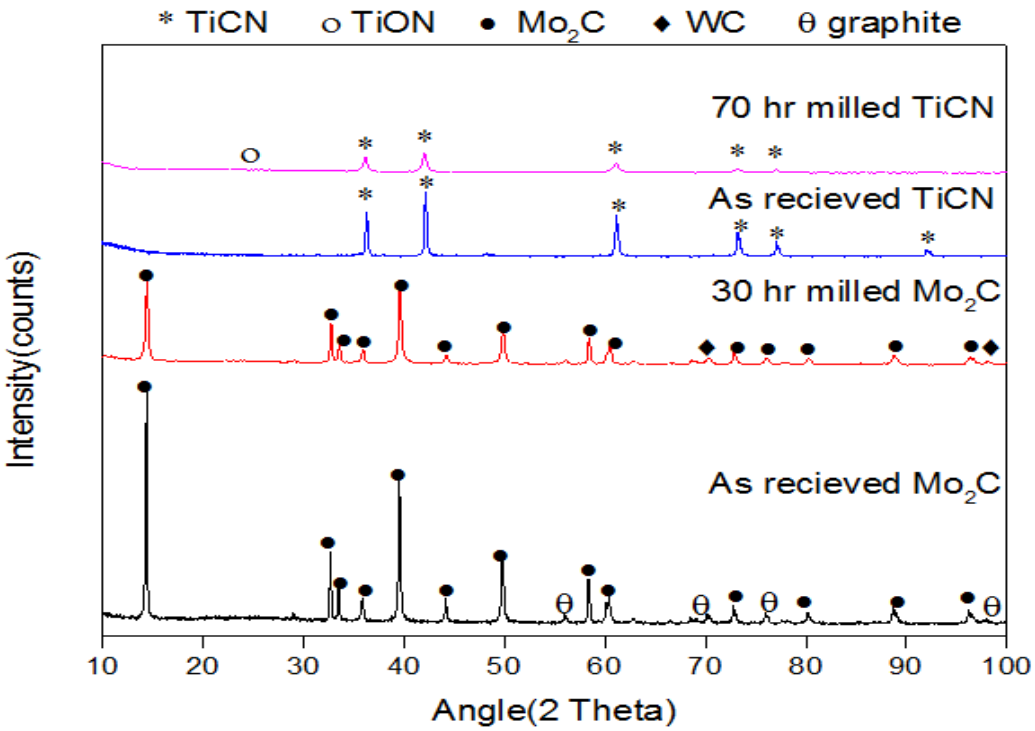

Fig. 4.8. XRD of ultrafine powders synthesized after ball-milling

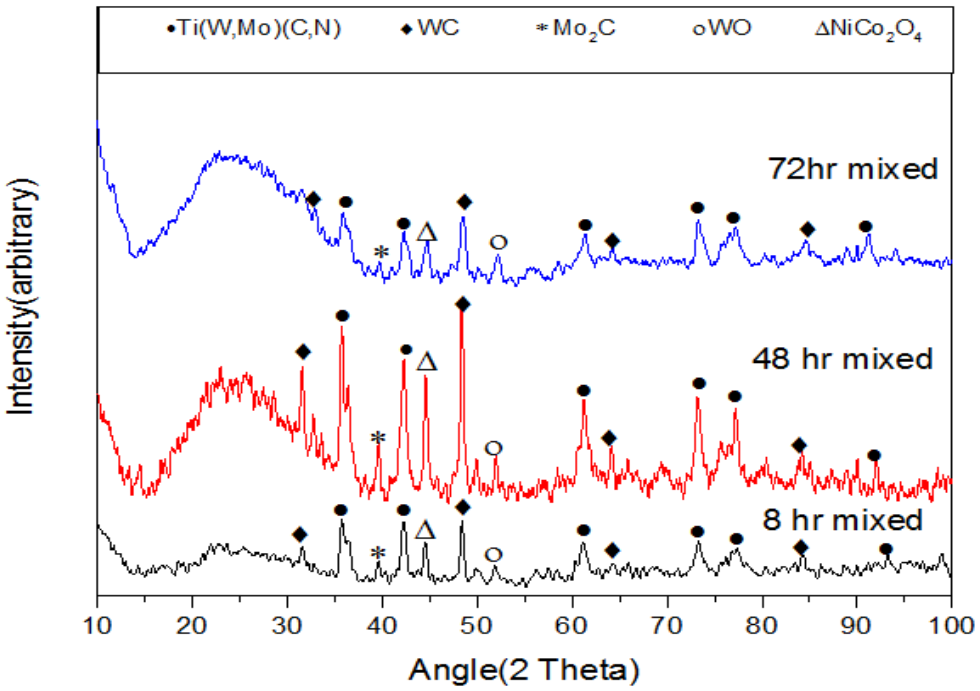

Fig. 4.9. XRD of ultrafine powders mixture

4.2 Spark plasma sintering results

Typical sintering profile for T8 cermets obtained from SPS in argon atmosphere is given in **Fig. 4.10**. The SPS parameters and corresponding obtained relative density is given in **Table 4.1**.

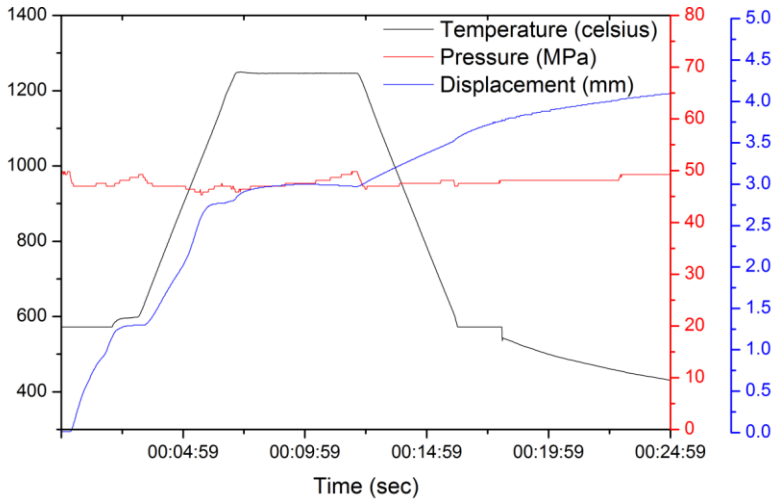

Fig. 4.10. Typical SPS sintered profile for T8 cermets

Table 4.1. T8 Cermets synthesized by SPS and sintering parameters

S.N.	Sample	SPS stages	SPS cycle				Relative density (%)
			Temperature (°C)	Pressure (MPa)	Heating rate (°C)	Holding time (min)	
1	T8	One	1300	55	200	2	97.10
2	**T8**	**One**	**1250**	**50**	**200**	**5**	**98.90**
3	T8	Two	1250 1100	50 40	200	3 5	95.80
4	**T8**	**Three**	**1100** **1000** **800**	**40**	**200**	**1** **3** **3**	**95.17**
5	T8	Three	1450 1000 800	30 40 40	50 75 100	5 5 5	97.58

Typical sintering profile for T48 cermets obtained from SPS in argon atmosphere is given in **Fig. 4.11**. The constant slope of the displacement curve after maximum temperature indicates full densification in the selected SPS conditions. The SPS parameters and corresponding obtained relative density is given in **Table 4.2**.

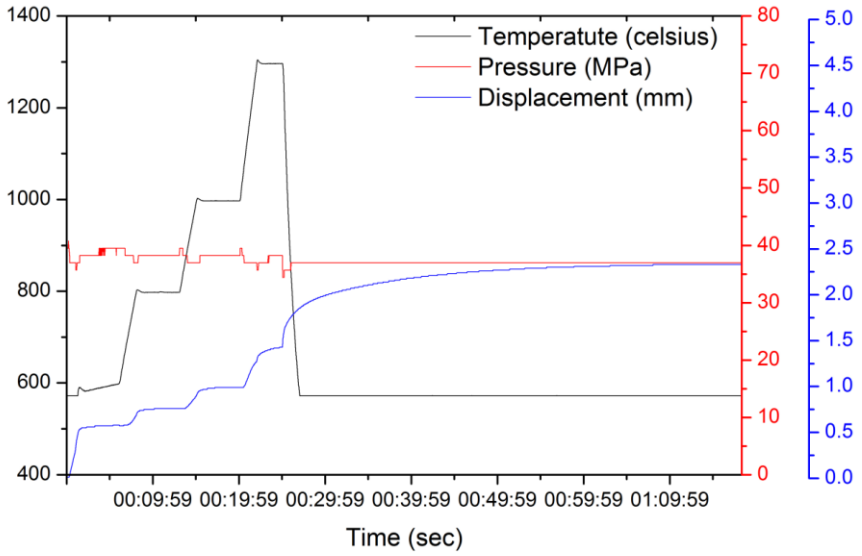

Fig. 4.11. Typical SPS profile for T48 cermets

Table 4.2. T48 Cermets synthesized by SPS and sintering parameters

S.N.	Sample	SPS stages	SPS cycle				Relative density (%)
			Temperature (°C)	Pressure (MPa)	Heating rate (°C)	Holding time (min)	
1	T48	Three	1250	40	200	3	91.37
			1000		100	5	
			800		100	5	
2	T48	Three	1400	40	50	2	98.27
			1000		75	3	
			800		100	3	
3	T48	Three	1300	40	200	3	100.00
			1000		100	5	
			800		100	5	

Typical sintering profile for T72 cermets obtained from SPS in argon atmosphere is given in **Fig. 4.12**. The constant slope of the displacement curve after maximum temperature indicates full densification in the selected SPS conditions. The SPS parameters and corresponding obtained relative density is given in **Table 4.3**.

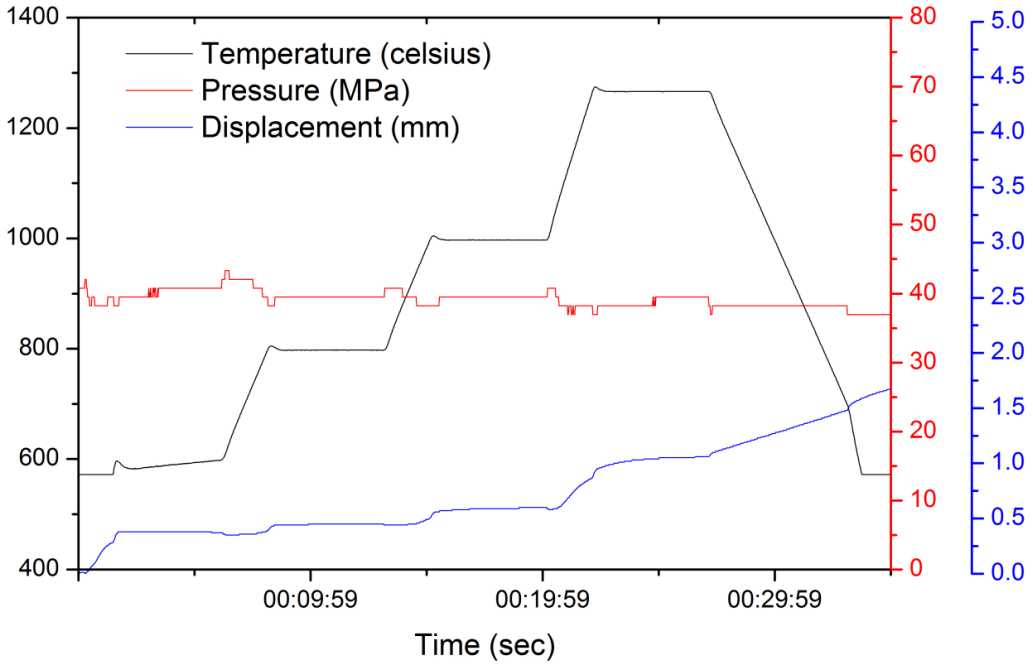

Fig. 4.12. Typical SPS profile for T72 cermets

Table 4.3. T72 Cermets synthesized by SPS and sintering parameters

S.N.	Sample	SPS stages	SPS cycle				Relative density (%)
			Temperature (°C)	Pressure (MPa)	Heating rate (°C)	Holding time (min)	
1	T72	Three	1270	40	200	5	94.48
			1000		100	5	
			800		100	5	
2	T72	Three	1200	40	200	3	98.27
			1000		100	5	
			800		100	5	

Typical sintering profile for T72 UHV cermets obtained from SPS in ultra high vacuum atmosphere is given in Fig. 4.13. The constant slope of the displacement curve after maximum temperature indicates full densification in the selected SPS conditions. The SPS parameters and corresponding obtained relative density is given in Table 4.4.

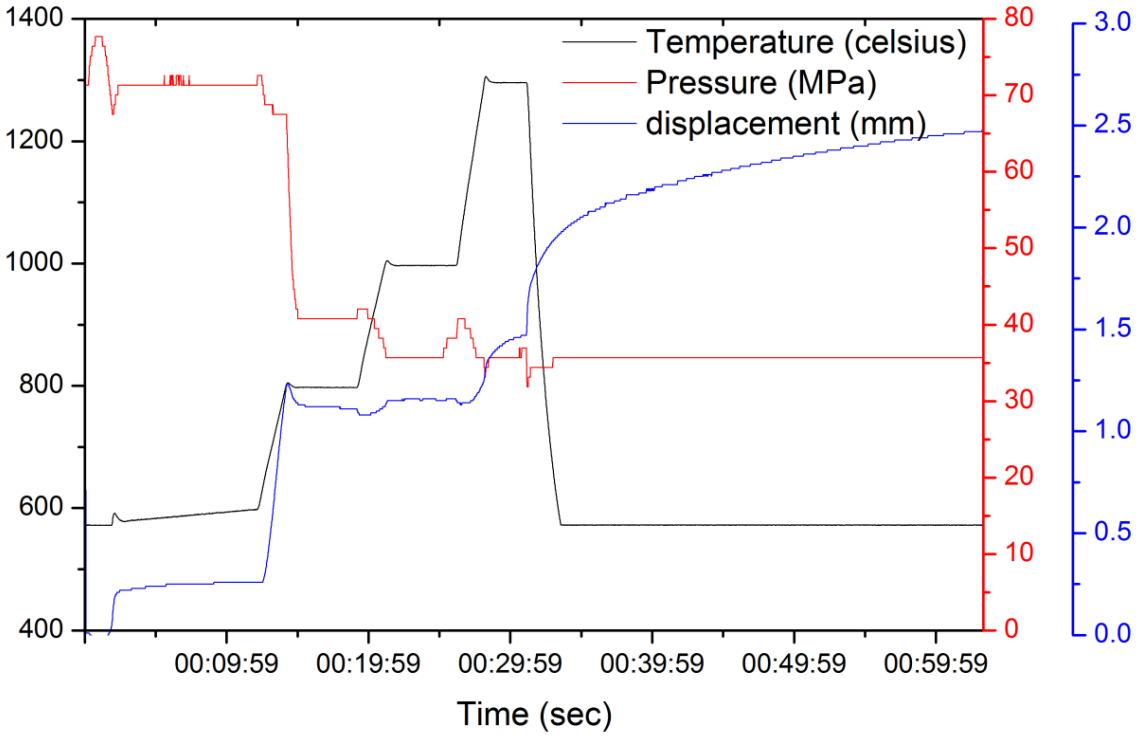

Fig. 4.13. Typical SPS profile for T72 UHV cermets

Basically, the effect of mixing i.e. the uniform mixing of particles in sintering is studied. The density increased in general with increase in mixing duration from 8 h to 72 h. The major peaks in XRD pattern were considered for the integrated intensities of peaks of respective phases and used for determining theoretical density of powder mixture. Accordingly, theoretical density is determined to be 5.85 g/cc. The same is explained below.

Table 4.4. T72 UHV Cermets synthesized by SPS and sintering parameters

S.N.	Sample	SPS stages	SPS cycle				Relative density (%)
			Temperature (°C)	Pressure (MPa)	Heating rate (°C)	Holding time (min)	
1	T72 UHV	Four	1300	40	100	3	93.44
			1000		100	5	
			800		100	5	
			600	70	50	20	
2	T72 UHV	Four	1300	40	100	3	95.80
			1000		100	5	
			800		100	5	
			600	70	50	20	
3	T72 UHV	Four	1300	40	100	3	98.31
			1000		100	5	
			800		100	5	
			370	70	25	30	

Integrated intensity of TiCN= 198; Integrated intensity of WC= 310

Integrated intensity of Mo_2C = 130; Integrated intensity of $W_{18}O_{49}$ = 19

Integrated intensity of $NiCo_2O_4$= 25; Total integrated intensities of peaks= 682

Volume fraction of $W_{18}O_{49}$ =19/682=0.0278

Volume fraction of $NiCo_2O_4$ =25/682=0.0366

$$\frac{1}{\rho} = \frac{x_{TiCN}}{d_{TiCN}} + \frac{x_{WC}}{d_{WC}} + \frac{x_{Mo2C}}{d_{Mo2C}} + \frac{x_{Ni}}{d_{Ni}} + \frac{x_{Co}}{d_{Co}} + \frac{x_{WO}}{d_{WO}} + \frac{x_{NiCoO}}{d_{NiCoO}}$$

……(4.1)

$$=(0.6/5.08)+(0.1/15.6)+(0.1/8.9)+(0.1/8.9)+(0.1/8.9)+(0.0278/8.33)+(0.0366/3.86) =0.1709$$

Theoretical density ρ = 5.85 g/cc

Highly dense (>97 %) samples obtained from sintering of 8h, 48 h and 72 h mixed powders are selected for further analysis.

4.3 Microstructure of as sintered sample

Fig. 4.14 shows BSE-SEM images of sintere cermets. Typically, sintered cermets consists of a black-core (Point A in **Fig.4.14**), white-core (Point of B in **Fig.4.14**), and grey-rim (Point R in **Fig.4.14**) type structures. According to the EDS analysis of points A, B and R and XRD analysis, it is confirmed that the core and the rim are both (Ti, W, Mo)(C, N) complex solid-solution, but differ in the Ti, W and Mo concentration. Schematic of as-sintered core-rim microstructure shown in **Fig.4.15**.

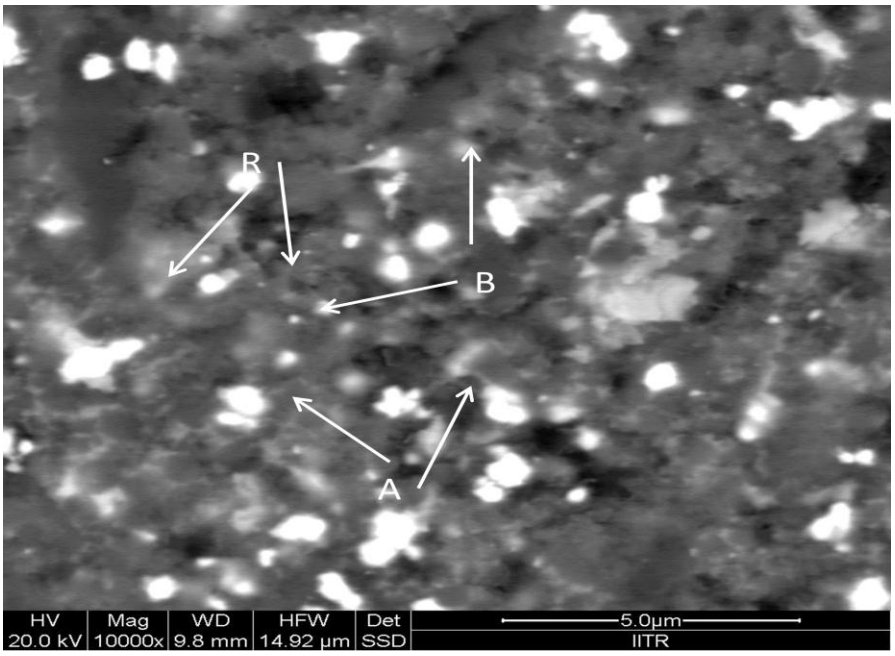

Fig. 4.14. Microstructure of as-sintered cermets showing core-rim structure

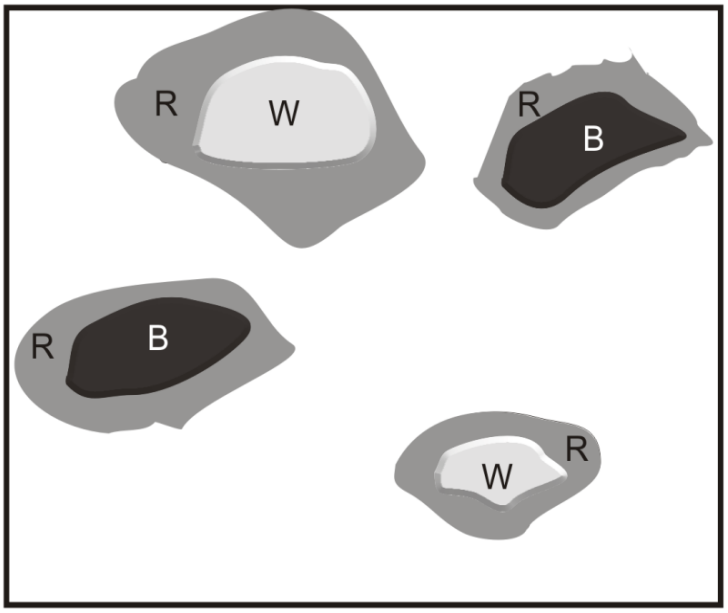

Fig. 4.15. Schematic of as-sintered Core-rim microstructure

4.4 XRD analysis of as sintered sample

XRD patterns of sintered cermets sample are shown in Fig. 4.16. XRD peaks shows that sample contains tungsten nitride (WN), tungsten oxide (WO) and cobalt-nickel oxide ($NiCo_2O_4$) peaks apart from Ti(W, Mo)(CN) cubic phase. Oxide phases were also found in the powders after mixing. The additional WN found in the sintered samples is possibly due to the nitridation of WC during sintering.

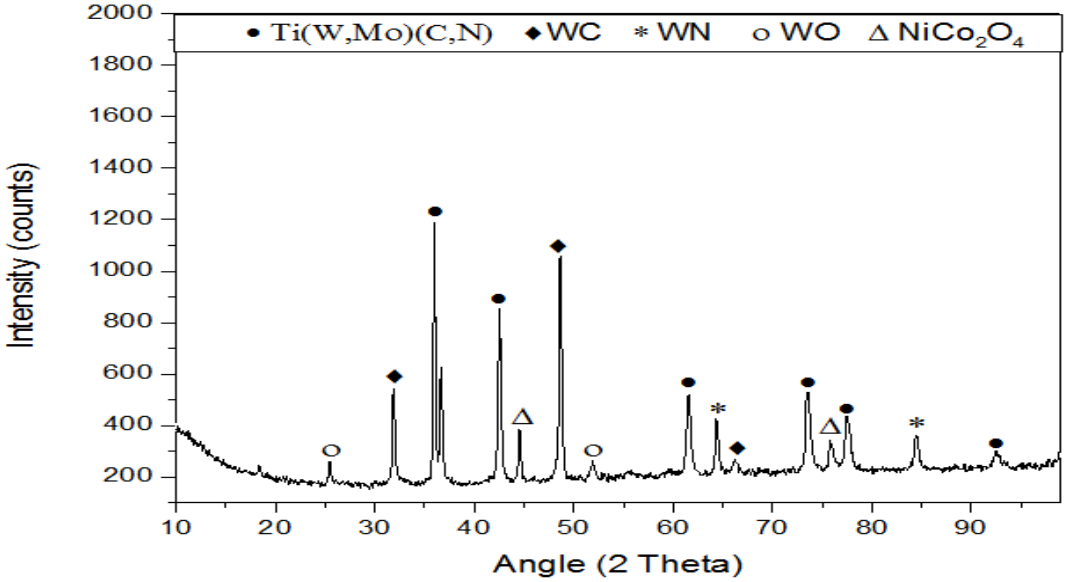

Fig. 4.16. XRD analysis of sintered sample showing WO, WN and $NiCo_2O_4$ phases

4.5 Mechanical properties

With increase in duration of mixing, the hardness increased. This can be attributed to the increase in density. A maximum hardness of 10.48 GPa is obtained for the cermets sintered using 72 h mixed powder, whereas a minimum hardness of 8.8 GPa obtained for the cermets sintered using 8 h mixed powder. Fracture toughness decreased from 9.44 MPa $m^{1/2}$ to 7.21 MPa $m^{1/2}$ with increase in mixing duration, **Table.4.5**.

Table 4.5. Mechanical properties of as-sintered cermets

S.N.	Sample	Relative density (%)	Hardness (GPa)	Fracture toughness ($MPam^{1/2}$)
1	T8	97.10	8.82 ± 0.58	9.44± 2.11
2	T48	98.27	9.6 ± 0.23	7.58± 3.05
3	T72	98.29	10.48 ± 0.20	7.21± 2.74

4.6 Erosion results

When prepared cermets eroded by SiC particles at normal incidence, the erosion rate decreased with increase in hardness of the sample. Fracture toughness has negligible influence on erosion of the cermets. With increase in temperature to 400^{o}C, the erosion rate increased by 1.5 to 2 times, **Table.4.6**.

Table 4.6. Erosion rate at RT and 400°C of as-sintered cermets

S.N.	Sample	Erosion rate ($mm^3/kg)*10^2$	
		RT	400°C
1	T8	1.41±0.055	2.96±0.68
2	T48	1.39±0.035	2.49±1.22
3	T72	1.37±0.025	2.44±0.27

4.7 Eroded surfaces

Typical worn surfaces of cermets sintered using 72 h (in **Fig. 4.17**).

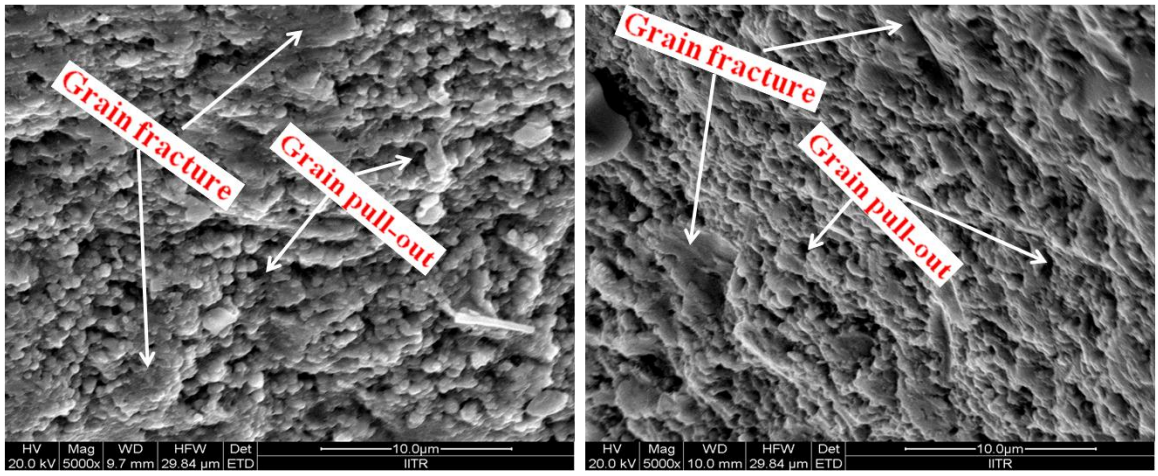

Fig. 4.17. Fracture surface of T72 cermets at (a) room temperature and (b) 400ºC.

In general, worn surfaces reveal removal of binder phase and pull-out or fracture of (Ti,W,Mo) grains during erosion. In elevated temperature erosion, the softened binder phase is easily removed and led to an increased fracture or pull-out of ceramic grains. The erosion results also indicate increased erosion rate for the samples tested at 400˚C.

In this study TiCN-10wt%WC-10wt% Mo_2C-10wt%Ni-10wt%Co powders mixture were prepared and sintered via SPS and characterized. The following results are investigated -

- Commercially available TiCN powders were ball milled to nano (<100 nm) size and Mo_2C powders to less than 300 nm. Powder mixtures of TiCN, 10% WC, 10%Mo_2C, 10 Ni and 10 %Co were uniformly mixed in ball mill. Contamination and oxidation are observed in mixed powders.
- Dense (>97%) TiCN-10wt%WC-10wt% Mo_2C-10wt%Ni-10wt%Co cermets were prepared by spark plasma sintering. Powders mixed for long time of 72 h resulted in highly dense cermets at 40- 50 MPa and 1250- 1300^oC for 3- 5 min in argon or vacuum.
- The microstructure of sintered cermets revealed distinct white core-back core-grey rim of (Ti, W, Mo)CN solid solution attached with Ni-Co. Typically, 10.48 GPa hardness and 9.44 MPa $m^{1/2}$ fracture toughness obtained for the 72 h mixed and spark plasma sintered sample.
- Erosion by SiC particles reveals removal of binder phase and pull-out or fracture of ceramic grains. Easy removal of binder phase at elevated temperature of 400^oC resulted in increased fracture of ceramic grains, leading to 1.5 to 2 times erosion compared to erosion at room temperature.

1. The oxidation during milling should be avoided to obtain good combination of properties of sintered TiCN-WC-Mo_2C-Ni-Co cermets. A proper reduction treatment of oxides is necessary and future work shall focus on sintering of reduced powder mixtures.
2. Parameters of spark plasma sintering are to be optimized to obtain cermets with high density and restricted coarsening to nano size for the new composition.
3. A systematic investigation on microstructural study involving crystallite size, contiguity etc. shall be done to understand the suitability of the newly developed TiCN-WC-Mo_2C-Ni-Co cermet.
4. In addition to hardness and fracture toughness, the rupture strength has also to be measured to understand the potential of the developed cermet.
5. Erosion performance can be studied at varied angles of impingement, velocity and particle size of erodent. Tests at elevated temperatures (800-1000°C) will be helpful in assessing the new cermet in high speed cutting or wear conditions. Sliding wear tests can also be done.

[1] Y. Peng, H. Miao, and Z. Peng, "Int . Journal of Refractory Metals and Hard Materials Development of TiCN-based cermets : Mechanical properties and wear mechanism," RMHM, vol. 39, pp. 78–89, 2013.

[2] S. Kang, "Some issues in Ti (CN) -WC- TaC cermets," vol. 209, pp. 306–312, 1996.

[3] S. Park and S. Kang, "Toughened ultra-fine (Ti , W)(CN)-Ni cermets," vol. 52, pp. 129-133, 2005.

[4] S. K. Seyed Mahdi Rafiaei, J.H. Kim, "Effect of nitrogen and secondary carbide on the microstructure and properties of $(Ti_{0.93}W_{0.07})$C-Ni cermets," Rmhm, vol. 44, pp. 123-128, 2014.

[5] A. Rajabi, M. J. Ghazali, J. Syarif, and A. R. Daud, "Development and application of tool wear: A review of the characterization of TiC-based cermets with different binders," Chem. Eng. J., vol. 255, pp. 445–452, 2014.

[6] J. Ihm, S. Kang, "A study of the formation of Ti (CN) solid solutions," vol. 47, no. 11, pp. 3241–3245, 1999.

[7] P. Ettmayer, H. Kolaska, W. Lengauer, and K. Dreyert, "Ti (C , N) Cermets - Metallurgy and Properties," vol. 13, pp. 343–351, 1995.

[8] Z. Lin, J. Xiong, Z. Guo, W. Zhou, W. Wan, and L. Yang, "Effect of Mo_2C addition on the microstructure and fracture behavior of (W,Ti)C-based cemented carbides," Ceram. Int., vol. 40 (10), pp. 16421–16428, 2014.

[9] J. Xiong, Z. Guo, B. Shen, and D. Cao, "The effect of WC , Mo_2C , TaC content on the microstructure," Materials & Design, vol. 28, pp. 1689–1694, 2007.

[10] J. M. Córdoba, E. Chicardi, R. Poyato, F. J. Gotor, V. Medri, S. Guicciardi, and C. Melandri, "Spark plasma sintering of $Ti_X\ Ta_{1-X}\ C_{0.5}\ N_{0.5}$ -based cermets : Effects of processing conditions on chemistry , microstructure and mechanical properties," vol. 230, pp. 558-566, 2013.

[11] Qian M. A. and L. C. Lim, "On the disappearance of Mo_2C during low-temperature sintering of Ti (C , N)-Mo_2C-Ni cermets," Journal of Materials

Science, vol. 4, pp. 3677-3684, 1999.

[12] R.M. Genga, L.A. Cornish and G. Akdogan, "Effect of Mo_2C additions on the properties of SPS manufactured WC-TiC-Ni cemented carbides," Int. Journal of Refractory Metals and Hard Materials, vol. 41, pp. 12–21, 2013.

[13] Y. Liu, Y. Jin, H. Yu and J. Ye, "Ultrafine (Ti, M)(C, N)-based cermets with optimal mechanical properties," Int. Journal of Refractory Metals and Hard Materials, vol. 29, pp. 104-107, 2011.

[14] Q. Xu, J. Zhao, X. Ai, W. Qin, D. Wang and W. Huang, "Effect of Mo_2C /(Mo_2C +WC) weight ratio on the microstructure and mechanical properties of Ti(C,N)-based cermet tool materials," Journal of Alloys and Compounds vol. 649, pp. 885-890, 2015.

[15] l.K. Yang and H.C. Lee, "Microstructural evolution during the sintering of a Ti(C,N)- Mo_2C-Ni alloy, Materials Science and Engineering A, vol. 209, pp. 213-217, 1996.

[16] D. Mari, S. Bolognini, G. Feusier, T. Cutard , C. Verdon , T. Viatte and W. Benoit, "TiMoCN-based cermets Part I. Morphology and phase composition," International Journal of Refractory Metals and Hard Materials, vol. 21, pp. 37-46, 2003.

[17] Z.A. Munir and U. Ansemlmi, "The effect of electric field and pressure on the synthesis and consolidation of materials: A review of the spark plasma sintering method," J. Mater. Science, vol. 41, pp.763-777, 2006.

[18] O. Guillon, J. Gonzalez-Julian, B. Dargatz, T. Kessel, G. Schierning, J. Rathel and M. Herrmann, "Field-Assisted Sintering Technology/Spark Plasma Sintering: Mechanisms, Materials, and Technology Developments", Advanced Engineering Materials, vol.33, pp. 830-849, 2014.

[19] P. Angerer, L. G. Yu, K.A. Khor, G. Korb and I. Zalite, "Spark-plasma-sintering (SPS) of nanostructured titanium carbonitride powders," vol. 25, pp. 1919-1927, 2005.

[20] Zgalat-lozynskyy, O., Herrmann, M., & Ragulya, "Spark plasma sintering of TiCN

nanopowders in non-linear heating and loading regimes," 31, 809, 2011.

[21] Feng Ping, Xiong Wei-hao, Zheng Yong, Yu Li-xin, Xia Yang-hua, "Spark plasma sintering properties of ultrafine Ti(C,N)-based cermet, Mater. Sci. Ed., Vol. 19, Issue 1, pp 69- 72, 2004.

[22] B.V. Manoj Kumar, J. Ram Kumar, Bikramjit Basu, "Crater wear mechanisms of TiCN-Ni-WC cermets during dry machining," International Journal of Refractory Metals & Hard Materials 25, 392–399, 2007.

[23] B.V. Manoj Kumar, Bikramjit Basu, "Mechanisms of material removal during high temperature fretting of TiCN–Ni based cermets," International Journal of Refractory Metals & Hard Materials 26, 504–513, 2008.

[24] A.Vijh, "On the influence of the magnitudes of metal-metal bond energies on the tribological parameters of metals," Wear, 79, 389-391, 1982.

[25] B.V. Manoj Kumar, J. Ramkumar, Bikramjit Basu, S. Kang, "Electro-discharge machining performance of TiCN-based cermets," International Journal of Refractory Metals & Hard Materials,vol.25,pp. 293–299, 2007.

[26] V. Monov, B. Sokolov, Stoenchev, "Grinding in Ball Mills : Modeling and Process Control I . Introduction," vol.12 (2), pp. 51–68, 2012.

[27] C. Suryanarayana, "Mechanical alloying and milling," Progress in Materials Science, vol.46 (1), pp.184-188, 2001.

[28] A.W. Weeber and H. Bakker, "Amorphization by ball milling: a review", Physica B,vol. 153, pp. 93–135, 1988.

[29] L. Takacs, "Self-sustaining reactions induced by ball milling," Progress in Materials Science, vol. 47, pp.355–414, 2002.

[30] J. Kübarsepp, , H. Klaasen, , J.Pirso, "Behaviour of TiC-base cermets in different wear conditions," Wear, vol.249, pp. 229-234, 2001.

[31] S. M. Shen, "Wear prediction of ceramics," Wear, vol. 256,pp. 867-878, 2004.

[32] U. Persson, H. Chandrasekaran, and Merstallinger, " Adhesion between some tool and work materials in fretting and relation to metal cutting,"Wear vol.249, pp. 293-301, 2001.

[33] P. Q. Campbell, J. Celis, Roos, V. Biest, "Fretting wear of selected ceramics and cermets," Wear vol.174,pp. 47-56, 1994.

[34] J. Gong, X. Gong, H. Miao, K. Zhao, "Effect of metallic binder content on the microhardness of TiCN-based cermets," Materials Science and Engineering, vol.359,pp.391-395, 2003.

[35] X. Zhang, N. Liu, R. Rong, " Effect of molybdenum content on the microstructure and mechanical properties of ultra-fine Ti (C , N) based cermets,"Materials Characterization, vol. 59, pp. 1690-1696, 2008.

[36] L. Chen, K. Kassel, "Fundamentals of liquid phase sintering for modern cermets and functionally graded cemented carbonitrides," International Journal of Refractory Metals & Hard Materials, vol. 18,pp. 307-322, 2001.

[37] Z. Xia, P. Shen, Z. Li," Mechanosynthesis of molybdenum carbides by ball milling at room temperature," Journal of Alloys and Compounds, vol. 453,pp. 185-190, 2008.

[38] H. Lee, "Microstructural evolution during the sintering of a Ti(C,N)- Mo2C-Ni alloy," Materials Science and Engineering, vol.209,pp. 213–217, 1996.

[39] S. Lee, H.S. Hong, H.S. Kimc, S.J. Hongc, J.H. Yoon, “Spark plasma sintering of WC-Co tool materials prepared with emphasis on WC core–Co shell structure development,” Int. Journal of Refractory Metals and Hard Materials, vol.53,pp. 41-45, 2015.

[40] Liu, C., N. Lin, Y. H. He, "Influence of Mo2C and TaC additions on the microstructure and mechanical properties of Ti (C , N)-based cermets," Ceramics International, vol.42, pp.3569-3574, 2016.

[41] S. Cardinal, A. Malchère, V. Garnier, G. Fantozzi, “Microstructure and mechanical properties of TiC-TiN based cermets for tools application,” Int . Journal of

Refractory Metals & Hard Materials, vol.27,pp. 521-527, 2009.

[42] M. Barsoum, edition 2nd, "Fundamentals of Ceramics," Mc Graw-Hill, New York, pp. 543-560,1977.